

**Absence of Saharan dust influence on the strontium isotope ratios on modern trees  
from the Bahamas and Turks and Caicos Islands**

Rick Schulting<sup>1</sup>, School of Archaeology, University of Oxford, UK

Mike Richards, Department of Archaeology, Simon Fraser University, BC, Canada

John Pouncett, School of Archaeology, University of Oxford, UK

Bryan Naqqi Manco, Caicos Pine Recovery Project Manager, Department of Environment  
and Coastal Resources, Turks and Caicos Islands

Ethan Freid, Bahamas National Trust/Leon Levy Native Plant Reserve, Bahamas

Joanna Ostapkowicz, School of Archaeology, University of Oxford, UK

---

<sup>1</sup> Corresponding author: [rick.schulting@arch.ox.ac.uk](mailto:rick.schulting@arch.ox.ac.uk)  
Telephone: +44 (0)1865 278309

## Abstract

We report on strontium ( $^{87}\text{Sr}/^{86}\text{Sr}$ ) isotope results from 91 modern trees growing on the Bahamas and Turks and Caicos Islands. The average  $^{87}\text{Sr}/^{86}\text{Sr}$  ratio of  $0.709169 \pm 0.000010$  is consistent with the late Quaternary limestone of the islands and with the modern ocean value. The absence of any detectable influence of  $^{87}\text{Sr}$ -enriched Saharan dust is notable, given the known contribution of this material to both past and recent soils of the Caribbean. Our results indicate that the impact of Saharan dust to the modern biosphere of the Bahamian archipelago is at least an order of magnitude less than modeled in currently available strontium isoscapes for the circum-Caribbean. We suggest that the bioavailability of Sr in Saharan dust may be considerably less than previously thought. Nevertheless, further work could usefully be carried out in the Bahamian archipelago on plants with different rooting depths, growing on different soil types and on limestone of different ages. Our results have particular relevance for the refinement of existing strontium isoscapes and the archaeological provenience of artifacts, animals and people in the circum-Caribbean.

Keywords: Caribbean; Bahamian archipelago; strontium isoscape; carbonate; Saharan dust

## INTRODUCTION

Atmospheric dust inputs are known to be an important factor affecting strontium isotope ( $^{87}\text{Sr}/^{86}\text{Sr}$ ) ratios in the biosphere. This makes the use of bedrock or surficial geological maps to predict  $^{87}\text{Sr}/^{86}\text{Sr}$  in living organisms potentially unreliable for provenience studies in both ecology and archaeology. In the circum-Caribbean, Saharan dust in particular is understood to have had a significant impact on development of paleosols on the Pleistocene terraces of carbonate islands exposed during periods of lowered sea levels (Muhs et al., 1990; Foos, 1991; Foos and Bain, 1995; Boardman et al., 1995; Borg and Banner, 1996; Herwitz et al., 1996). This dustfall continues into the present, and is an important source of mineral nutrients for the Caribbean basin's biosphere (Delaney et al., 1967; Prospero and Carlson, 1972; Prospero and Nees, 1986; Goudie and Middleton, 2001; Formenti et al., 2011; Prospero and Mayol-Bracero, 2013). Its contribution is of particular relevance to the mineral-impoverished, high-purity carbonate islands of the Bahamian archipelago. Because of its relatively high  $^{87}\text{Sr}/^{86}\text{Sr}$  ratio, Saharan dust would be expected to have an influence on the isotopic composition of vegetation, as has been recently modeled in a strontium isoscape for the Caribbean (Bataille et al., 2012; Laffoon et al., 2012).

In this paper, we present the results of a program of  $^{87}\text{Sr}/^{86}\text{Sr}$  measurements on modern trees (primarily *Swietenia* sp. and *Guaiacum* sp.) from the Bahamas ( $n = 37$ ) and the Turks and Caicos Islands (TCI) ( $n = 54$ ) (Figure 1). To our knowledge these are the first such data to be reported from the terrestrial biosphere of these islands. The aim is to determine the extent to which modern  $^{87}\text{Sr}/^{86}\text{Sr}$  measurements are influenced by legacy and ongoing allochthonous inputs, the most important of which is expected to be Saharan dust (others

include sea-spray, volcanic ashfall, and dust from the Mississippian loess belt). Our study builds on previous work in the region, and serves in part as a test of the predictions made by Bataille et al.'s (2012) strontium isoscape. Ultimately, the intention is to use these data in conjunction with other isotopic datasets being produced in the circum-Caribbean, to facilitate studies of the origins and mobility of pre-Columbian humans, animals and artifacts (Laffoon et al., 2012; 2014; 2016; 2017; Ostapkowicz et al., 2017). The results may also be of interest to those creating isoscapes in other parts of the world (Evans et al., 2010; Snoeck et al., 2016) and to those studying pedogenesis and soil processes using Sr as a tracer for calcium cycling (e.g., Åberg et al., 1990; Reynolds et al., 2012).

### **Strontium isotope studies in the circum-Caribbean**

Strontium (Sr) is an alkaline earth metal with four naturally occurring isotopes,  $^{84}\text{Sr}$  (0.56%),  $^{86}\text{Sr}$  (9.86%),  $^{87}\text{Sr}$  (7.00%), and  $^{88}\text{Sr}$  (82.58%) (Faure, 1986). The most important of these for provenience studies is  $^{87}\text{Sr}$ , deriving from the  $\beta$  decay of rubidium ( $^{87}\text{Rb}$ ). Thus, the ratio of  $^{87}\text{Sr}/^{86}\text{Sr}$  will depend on the amount of rubidium originally found in the rock, and the passage of deep time (Faure, 1986). In a Caribbean context, young geological formations such as those of the volcanic arc of the Lesser Antilles can have  $^{87}\text{Sr}/^{86}\text{Sr}$  ratios as low as 0.704, while those of older sedimentary and metamorphic formations will have higher ratios of up to 0.715 (e.g., Pushkar et al., 1973; Borg and Banner, 1996; Laffoon et al., 2012; Ostapkowicz et al., 2017). Most ratios, including those of marine carbonates, fall between these extremes. Strontium becomes incidentally incorporated in lieu of calcium into the tissues of a tree (or other plant) when taken up in solution during the course of the tree's life (Faure, 1986; Capo et al., 1998). It will therefore reflect the bioavailable  $^{87}\text{Sr}/^{86}\text{Sr}$

ratio of that location, which in turn will be comprised of a combination of Sr from a number of sources, the most important of which will usually be bedrock weathering.

The surface exposures of the Bahamian archipelago (comprising the Bahamas and TCI) are composed entirely of Quaternary limestone, with the most widespread deposits being those of the late Pleistocene Grotto Beach Formation (Marine Isotope Stage 5e) (Carew and Mylroie, 1985; 1995; Mylroie and Carew, 1995; Carew and Mylroie, 1997; Mylroie et al., 2012; see also Wanless et al., 1989 for TCI), dating to 132–119 ka (Chen et al., 1991). This in turn is often overlain by lithified intertidal and aeolian-derived deposits of the Holocene Rice Bay Formation (Mylroie and Carew, 1995; Carew and Mylroie, 1997). While  $^{87}\text{Sr}/^{86}\text{Sr}$  ratios exhibit a more or less linear increase over the course of the Pleistocene, no trend is readily apparent for the last 130 ka, during which time ratios do not depart significantly from the contemporary ocean value of ca. 0.70917 (Capo and DePaolo, 1990; Hodell et al., 1990; Dia et al., 1992; Henderson et al., 1994; McArthur, 1994), although slightly higher values of ca. 0.70920 have also been reported (Kuznetsov et al., 2012). While middle Pleistocene deposits have long been recognized in the Bahamas (Owl's Hole Formation), they are almost always overlain by late Pleistocene deposits, and are usually exposed only on sea cliffs or in modern road cuts and quarries (Carew and Mylroie, 1985; 1995; Hearty and Kindler, 1993; 1997; Hearty, 1998). The Miocene and early Pleistocene deposits recently identified along the north coast of the island of Mayaguana have not yet been recognized elsewhere in the archipelago (Kindler et al., 2011). Strontium isotope ratios on middle Pleistocene (0.34–0.88 Ma) carbonate samples from the island average  $0.709155 \pm 0.000009$  ( $n = 4$ ), significantly lower than the abovementioned late Pleistocene value of ca. 0.70917.

The  $^{87}\text{Sr}/^{86}\text{Sr}$  ratio of ca. 0.70917 for modern seawater is closely comparable to that observed in a range of marine taxa (gastropods, bivalves, foraminifera, echinoderms, algae and coral) on Lee Stocking Island, Bahamas, spanning habitats from the coral reefs to mangrove swamps, averaging  $0.709179 \pm 0.000012$  ( $n = 40$ ) and confirming the absence of vital effects, i.e., fractionation (Reinhardt et al., 1999). However, the relationship of bioavailable Sr to the local geology is not always straightforward, especially in terrestrial systems (Sillen et al., 1998, Evans et al., 2010; Hartman and Richards, 2014; Snoeck et al., 2016), being affected by a combination of weathered Sr from the underlying bedrock (Bain and Bacon, 1994), Sr deposited in rainfall and sea-spray (Vitousek et al., 1999; Whipkey et al., 2000; Montgomery et al., 2003; Hodell et al., 2004; Evans et al., 2010), as well as Sr in wind-borne dust and soil particles (Prospero et al., 1981; Reynolds et al., 2012). The potential impact of Saharan dust on the Bahamian archipelago's biosphere is clear from its  $^{87}\text{Sr}/^{86}\text{Sr}$  ratio of ca. 0.716–0.718 (Grousset and Biscaye, 1989; 2005; Grousset et al., 1992; Rognon et al., 1996), which is considerably higher than that of ca. 0.7092 for late Quaternary limestone. The extent of its impact will depend on the relative amounts of Sr found in these two sources and on their bioavailability.

Saharan dust has been identified as an important contributor to both past and present soils from the Lesser Antilles to Florida, with its strongest expression in the so-called 'red soils' that formed during Pleistocene stadials (Delaney et al., 1967; Syers et al., 1969; Prospero and Nees, 1986; Prospero et al., 1987; Muhs et al., 1987; 1990; Borg and Banner, 1996; Prospero, 1999; Kamenov et al., 2009). Prospero and Mayol-Bracero (2013) refer to the Caribbean basin as a major "receptor" site for Saharan dust, which accounts for over half of modern global dust emissions. It has been estimated that some 30 to 50 million tonnes of Saharan dust falls on the Caribbean annually (Prospero and Carlson, 1972; Colcaro et al.,

2003; Kaufman et al., 2005; see also Prospero et al. 1987). On the basis of a detailed geochemical study of paleosols from Barbados, the Bahamas, and the Florida Keys, Muhs et al. (1990:171; see also Muhs et al., 2007) state that “Saharan dust has been the major parent material for soils on Quaternary limestones of Caribbean and western Atlantic islands in the last 900,000 yr”. Moreover, it is now widely accepted that it is difficult to develop soils on young limestone islands from bedrock dissolution alone, again emphasizing the importance of atmospheric dust sources, including Mississippi River Valley loess, volcanic ash and Saharan dust (Syers et al., 1969; Bricker and Mackenzie, 1970; Muhs et al., 1987; 1990; Boardman et al., 1995; Prognon et al., 2011). For the western Caribbean specifically, the contribution of volcanic dust has been shown to be negligible, and, while Mississippian loess may be a minor contributor in the more northern islands, the dominant source is clearly North African dust (Muhs et al., 2007).

There have been a number of studies from a range of disciplines employing Sr isotopes in the circum-Caribbean region. Recently, there has been considerable interest from the archaeological community in the use of strontium and other isotopes to trace the provenience of artifacts, animals and people (Laffoon and Hoogland, 2012; Laffoon et al., 2012; 2014; 2016; 2017; Ostapkowicz et al., 2012; 2013; 2017; Pestle et al., 2013). Bataille et al. (2012) have developed a sophisticated Sr isoscape taking into account the contributions of island bedrock geology, differential weathering of rock types, rainfall and atmospheric dust deposition. However, the availability of biologically available baseline data to validate their model is still spatially patchy. In particular, the model includes no data relating to the terrestrial environment of the Bahamas/TCI.

Here, we present strontium isotope data on 91 modern trees from seven islands spanning some 600 km of the Bahamian archipelago, to assess whether any isotopically distinct allochthonous inputs can be detected. Previous studies have suggested that highly weatherable carbonate bedrock will dominate over the contribution of  $^{87}\text{Sr}$ -enriched Saharan dust, though not override it entirely (Bataille et al., 2012:13, Fig. 5; see also Bern et al., 2005). Thus, the extent of the latter's potential impact is unclear. While carbonate bedrock will undergo high rates of weathering, in the absence of a developed soil containing clay minerals, this material will not be retained. Balancing this, Saharan dust is an annual input. Furthermore, vegetation itself acts as a dust trap, with subsequent throughfall supplying further aeolian sediments to the soil (Graustein and Armstrong, 1983; Lovett and Lindberg, 1984; Gosz and Moore, 1989; Åberg et al., 1990; Reynolds et al., 2012).

By the time it reaches the Caribbean, deposition of Saharan dust is mainly through wet removal processes, with dust particles acting as cloud condensation nuclei (Nowottnich et al., 2011). This is particularly relevant to our study in that the Bahamas not only receive substantially higher annual precipitation than TCI (800-1100 mm/yr vs. 400-800 mm/yr), but rainfall is concentrated in the summer months in the former, versus the winter months in the latter (Sears and Sullivan 1978; Whitaker and Smart, 1997) (Figure 2). Because Saharan dust transport to the Caribbean occurs primarily in the summer months (Prospero et al., 1981; Prospero, 1999; Goudie and Middleton, 2001; Colcaro et al., 2003; Prospero and Lamb, 2003; Prospero et al., 2014), we might expect the Bahamas to receive higher inputs of Saharan dust than TCI. Counteracting this, and responsible for the opposite trend modeled by Bataille et al. (2012: Fig. 5) is the reduced bedrock weathering resulting from lower average rainfall in the southern archipelago (including TCI), but, as acknowledged by



the authors, this does not take into account the potential impact of the strong seasonal bias resulting from the combination of summer precipitation and the presence of Saharan dust. There is a clear precipitation gradient even within the Bahamas that is partly captured by our dataset, with Long Island to the south receiving approximately half the rainfall of Cat Island and Eleuthera to the north. This effect increases in the northern Bahamian islands, culminating in Andros, where summer rainfall is twice as high as on Eleuthera. Unfortunately our study does not include samples from the northern islands. Though the atmospheric dust sources differ from those being considered here, it is worth noting that Gosz and Moore (1989) demonstrated a marked seasonal shift in  $^{87}\text{Sr}/^{86}\text{Sr}$  ratios in precipitation in the mountains of New Mexico. This effect has yet to be demonstrated empirically for our study region, but underlies one of our research questions.

We test the following hypotheses:

- 1) Saharan dust will have a small but detectable effect on trees growing on the Bahamian archipelago, raising  $^{87}\text{Sr}/^{86}\text{Sr}$  ratios above those of the late Quaternary deposits, as modeled by Bataille et al. (2012: Fig. 5B).
- 2) The impact of Saharan dust may exhibit an increasing southeast to northwest gradient, paralleling the summer precipitation gradient, when atmospheric dust of North African origin is also at its peak (thus, we are testing the reverse of the pattern expected from Bataille et al.'s model in this respect, for reasons discussed above).
- 3) The impact of Saharan dust may be greater in smaller trees with shallower rooting systems, whereas larger trees with deeper rooting systems will be dominated by bedrock  $^{87}\text{Sr}/^{86}\text{Sr}$  ratios (Reynolds et al., 2012; Hartman and Richards, 2014; though see Poszwa et al. (2002) who found that deep roots contributed little or no Sr to trees in a tropical

rainforest, but that instead there is a focus on the uppermost soils where fine rootlets concentrate to take advantage of nutrients from leaf litter).

4) The impact of Saharan dust may differ according to topography and/or elevation, with less accumulation on ridges as opposed to planes and other low-lying areas and swales ('channels') having greater potential for the accumulation of dust over recent time as well as tending to be foci for lateritic 'red soil' paleosols (Little et al., 1977: 54; Wanless et al., 1989: 53).

5) The impact of Saharan dust will be marginally higher in 'inland' areas, here defined as lying more than 1km from the coast, since these are more protected from coastal erosion and so may have greater soil depth.

6) The impact of Saharan dust will be greater in trees growing on clay-rich loams, particularly the 'red soils' derived from Saharan dust, than those growing on coral sands.

Note that (5) and (6) are not independent, since the coral sands are primarily coastal though on occasion they do extend 'inland' by more than 1km. While the effects in all cases are expected to be small because of the predominant contribution of carbonate bedrock-derived Sr, our relatively large sample size together with the isotopic homogeneity of the islands' late Quaternary bedrock deposits should enable us to detect even slight shifts towards higher  $^{87}\text{Sr}/^{86}\text{Sr}$  ratios, should they exist. Thus, the Bahamian archipelago is well suited for testing the potentially subtle effects of Saharan dust on  $^{87}\text{Sr}/^{86}\text{Sr}$  ratios in living vegetation growing over carbonate bedrock in the western Caribbean.

## **MATERIALS AND METHODS**

Ninety-one samples from living trees were collected in 2009 from Eleuthera (n = 2), Cat Island (n = 15) and Long Island (n = 20) in the Bahamas, and from Providenciales (n = 12) and North (n = 21) Middle (n = 14) and East Caicos (n = 7) in TCI (Figures 1, 3–4). The majority of the samples collected were of *Guaiacum sanctum* (n = 44) and *Swietenia mahagoni* (n = 36), since these taxa have been identified as among the most commonly used for pre-Columbian woodcarvings in the Bahamas and TCI (Ostapkowicz et al., 2012; Ostapkowicz, 2015). Smaller numbers of samples of *G. officinale* (n = 4), *Zanthoxylum flavum* (n = 4), *Cordia sebestina* (n = 2) and *Lysiloma latisiliquum* (n = 1) were also collected; these species too are known to have been used in pre-Columbian woodcarving. One of the original aims of this project was to develop baseline data for the interpretation of  $^{87}\text{Sr}/^{86}\text{Sr}$  ratios obtained on these artifacts (Ostapkowicz et al., 2012), and using the same taxa for the modern study removed a potentially confounding variable. *Guaiacum* and *Swietenia* are CITES-listed (Convention on International Trade in Endangered Species), and the project fully complied with all regulations pertaining to the documentation and export/import of specimens (CITES permit nos. 2009/356 [Bahamas] and PLS-W-2009-39, 417091/01 [Turks and Caicos]). As part of the agreement with the national agencies, botanical specimens were collected from the same trees, and were dried and prepared for herbarium collections in national institutions in the Bahamas and TCI, with another archive held in the World Museum Liverpool. Field sampling was undertaken with botanists from the National Trusts of the Bahamas (EF) and Turks and Caicos Islands (BNM), who provided in-field species identifications.

Potentially relevant is the rooting depth of these genera—among the largest indigenous trees on the islands—which could tap into the rare deeper soils that include aeolian inputs accumulated over decades or more, or, alternatively, beneath the shallow soil horizon

entirely into carbonate bedrock, whereas shallow-rooting plants might predominantly reflect leaf litter and more recent inputs over the last few years. However, over-harvesting of *Guaiacum* and *Swietenia* in the 17-19<sup>th</sup> centuries has left few surviving groves in the Bahamas and TCI (Correll and Correll, 1982:26). Most are found in what is known locally as ‘coppice’ wood, and many take the form of bushes rather than full size trees. In any case, a study by Pozwa et al. (2002) suggests that in nutrient-poor soils—which certainly describe the Bahamian archipelago—Sr uptake will focus on the near-surface layer. Moreover, soils across the study region are generally thin, often only a few centimeters over bedrock, though some solution holes (‘banana holes’) have become infilled to depths of a few meters (Mooney, 1905; Little et al., 1977).

Once a grove or individual tree was identified, GPS coordinates and detailed information on tree size and environment were documented, and each sampled tree was photographed. Twigs of ca. 1 cm in diameter were taken from trees ranging in height from ca. 1 to 12m (averaging ca.  $4.1 \pm 2.0$ m), and from ca. 0.05 to 0.5m in diameter at chest height (averaging ca.  $0.25 \pm 0.10$ m). Only the branchwood was used for Sr isotope analysis, and so reflects growth over a period of 2-4 years. For the purposes of analysis, trees were divided into three size classes: small (0.05–0.20m diam at chest height, 1.0–3.0m height), medium (0.20–0.40m diam, 3.0-5.0m height) and large (>0.40m diam, >5.0m height). Appropriate size information was recorded for 86 trees (measurements for five trees were not recorded).

Collection sites were chosen to provide wide coverage of the selected islands (which were themselves chosen based on the known presence of the target tree species) to investigate possible subtle differences in Sr isotope ratios, e.g., between coast and interior, defined as

<>1km from the coast, respectively, and between landforms. This coast-inland division was chosen primarily because transects on both the west and east coasts of Ireland suggest that the effects of sea-spray on  $^{87}\text{Sr}/^{86}\text{Sr}$  ratios in the biosphere do not extend past 1km on carbonate bedrock (Snoeck, 2014). This is in contrast to other studies reporting stronger and more widespread impacts of sea-spray and/or rainfall (Vitousek et al., 1999; Whipkey et al., 2000; Montgomery et al., 2003; Hodell et al., 2004), but these studies refer to regions dominated by basaltic or granitic bedrocks that are far more resistant to weathering than limestone, and so are more readily affected by allochthonous inputs (cf. Bataille et al., 2012).

Morphometric characterization of landform at the sample locations was carried out using 1 arc second (ca. 30m at the equator) Shuttle Radar Topography Mission (SRTM) void-filled digital elevation model<sup>1</sup> in Landserf 2.3.1 (Wood, 2009). Cells in a digital elevation model can be classified as pits, channels, passes, ridges, peaks or planes using unique criteria based on four surface parameters: slope, cross-sectional curvature, maximum curvature and minimum curvature (Wood, 1996). Surface parameters are calculated using quadratic approximation, fitting a quadratic trend surface through all of the data points corresponding to the cells in an  $n \times n$  window and calculating the values of the parameters for the cell at its centre. The values of the surface parameters and the subsequent characterization of the morphometric feature types are scale dependent, i.e. dependent on the size of the  $n \times n$  window. Multiscalar characterization can be performed by calculating fuzzy feature classes, with values for each morphometric feature type ranging between 0 (not classified as that feature type at any scale of analysis) and 1 (classified as that feature type at all scales of analysis). Fuzzy feature classes were calculated for the Bahamas and

---

<sup>1</sup> <https://lta.cr.usgs.gov/SRTMVF>

Turks and Caicos Islands for window sizes between 3 and 31, equivalent to planimetric distances of between c.100m and c.1km. Dominant feature types for the sample locations were determined on the basis of the fuzzy feature class with the highest value (ridges, n = 11; planes, n = 74, and; channels, n = 3). The fuzzy feature classes for the sample locations were also reclassified as negative features (pits > 0 or channels > 0 or passes > 0) or positive features (ridges > 0 or peaks > 0) in order to determine locations where sediments were likely to accumulate and locations where erosion was likely to have occurred (negative, n = 21, and; positive, n = 35<sup>1</sup>).

We have soil maps only for Long and Cat Islands (we have been unable to source any from TCI), and have plotted sampling locations against areas identified as Bahama Black Loam (n = 18), Bahama Red Loam (n = 5), Coral Sands (n = 10) and Brackish Swamp (n = 2) (Mooney 1905) (Figure 5). Field observations suggest that the two locations on what were identified as 'Brackish Swamp' in the early 20<sup>th</sup> century may have since been drained as part of now largely abandoned attempts to improve soil fertility for agriculture (Little et al., 1997). The designation is retained here, since there may be a legacy effect on these soils. The lateritic clay-rich 'Red Loam' represents exposed Pleistocene paleosols with high concentrations of Saharan dust. They can range in color from deep red (Munsell 10Y 2/2) to light yellow-brown (10YR 7/6), mainly reflecting diagenetic processes (Foos and Bain, 1995). Unfortunately these are the least well represented in our study, since testing soil differences was not an original aim of the project. Nevertheless, because Saharan dustfall is an annual input, its contribution might be reasonably expected to feature in all soils to some extent (Prospero and Carlson, 1972; Colcaro et al., 2003; Kaufman et al., 2005;

---

<sup>1</sup> Locations that were classified as positive features at one or more scales of analysis and negative features at one or more scales of analysis were excluded from these counts.

Prospero and Mayol-Bracero, 2013). The contribution of Saharan dust to other soils in the Bahamas is confirmed by its presence in trace amounts even in coral sands (Foos and Bain, 1995). Furthermore, the relatively organic-rich 'black soils' that dominate our sampling locations—in addition to containing the Sr taken up by decomposing plants during life—should also trap and hold the Saharan dust that continues to fall each summer. This is because strontium cations ( $\text{Sr}^{2+}$ ) will be relatively strongly adsorbed onto negatively charged clay minerals and organic matter (Capo et al., 1998:201, 208). Indeed, pre-Holocene peat samples from San Salvador and Andros were found to contain significant amounts of boehmite, a marker for Saharan dust (Boardman et al., 1995:44), clearly demonstrating that the latter's impact is not restricted to the 'red soils'.

A caveat in terms of the application of our findings to the pre-Columbian period is that the soils of the Bahamian archipelago have been heavily eroded following deforestation in the early colonial period and so may not fully reflect the earlier situation. The transport of Saharan dust over the Caribbean has also varied over time, particularly as a result of precipitation over the Sahel and of the strength of winds over the dust source regions (Prospero and Lamb, 2003; Ridley et al., 2014). Nevertheless, data from 2002–2011, encompassing sample collection in July 2009, shows that these years all recorded substantial summer Saharan dustfall in the Caribbean (Prospero et al., 2014: Fig. 7).

### **Strontium isotope analysis**

Branchwood samples were prepared for Sr isotope analysis following methods outlined in Reynolds et al. (2005). Samples ranging in size from 20 to 100mg were first cleaned in ultrapure water and then ashed at 850° before being prepared following standard Sr

isotope preparation procedures and measurement using a ThermoFinnigan Neptune Inductively-Coupled Plasma Multi-Collectors Mass Spectrometer (MC-ICP-MS) at the Department of Human Evolution, Max Planck Institute of Evolutionary Anthropology, Leipzig, Germany (see details in Copeland et al., 2008). For quality assurance, measurements runs included the international Standard Reference Material (SMR) 1486, and samples were corrected using the SRM 987 strontium carbonate isotopic standard (<https://www.nist.gov/srm>). Measurement errors are on the order of +/- 0.00003, based on long-term repeat analyses of SRM 1486 at the Max Planck Institute.

Statistical tests were carried out in SPSS. Data were assessed for normality and parametric or nonparametric tests were applied as appropriate (the latter were not required). Heteroscedastic tests were applied in cases when variance was not homogeneous.

## RESULTS

The  $^{87}\text{Sr}/^{86}\text{Sr}$  isotope ratios obtained on 91 samples are extremely homogeneous, with a mean of  $0.709169 \pm 0.000010$  and a coefficient of variation of only 0.001% (Tables 1 and 2; Figure 6). The data are normally distributed (Shapiro-Wilk test,  $W = 0.983$ ,  $p = 0.295$ ), with only four samples lying more than two standard deviations from the mean (see Z-scores in Table 1); this is approximately what would be expected given the sample size. In terms of the hypotheses set out in the paper:

1) There is no detectable  $^{87}\text{Sr}$ -enrichment as a result of Saharan dust, as the overall mean of  $0.709169 \pm 0.000010$  is indistinguishable to five decimals places from modern seawater (Hodell et al., 1990; Dia et al., 1992; Henderson et al., 1994; McArthur, 1994).



366 2) There is no difference between the means of the island groups, with the Bahamas  
 367 averaging  $0.709170 \pm 0.000007$  ( $n = 37$ ) and TCI averaging  $0.709168 \pm 0.000012$  ( $n = 54$ )  
 368 (heteroscedastic Student's  $t$ -test,  $t = 0.96$ ,  $p = 0.34$ ). However, the TCI results are  
 369 significantly more variable (F-test,  $F = 2.46$ ,  $p = 0.005$ ), including the four highest and seven  
 370 lowest measurements in the dataset (Figure 6). There are no differences in the means of  
 371 the individual islands independent of island group (ANOVA,  $F = 0.31$ ,  $p = 0.93$ ,  $df = 6, 83$ ).  
 372 Together, these two tests also act as a proxy for assessing the postulated positive  
 373 relationship with summer precipitation, for which no evidence is seen. This also tests for  
 374 the east to west pattern of decreasing impact of Saharan dust modelled by Bataille et al.  
 375 (2012), and again no such trend can be observed.

376 3) There is no difference between the three tree size classes (ANOVA  $F = 0.18$ ,  $p = 0.84$ ,  $df =$   
 377  $2, 83$ ). No difference between tree species was anticipated, since samples from the two  
 378 main species targeted each reflect the full range of tree size and so would be expected to  
 379 have similar rooting depth, nor do they have different habitat requirements, and indeed are  
 380 sometimes found growing near one another (e.g., Figure 3b, samples L16 and L17). The  
 381 lack of any effect in this regard was confirmed (ANOVA,  $F = 1.07$ ,  $p = 0.36$ ,  $df = 3, 84$ ).

382 4) There is no difference by topographical location (planes, ridges and channels: ANOVA,  $F$   
 383  $= 0.34$ ,  $p = 0.71$ ,  $df = 2, 85$ ; negative and positive positions: Student's  $t$ -test,  $t = 1.17$ ;  $p =$   
 384  $0.25$ ;  $df = 54$ ), or elevation (linear regression model,  $r^2 = 0.00$ ,  $p = 0.52$ ,  $n = 88$ ).

385 5) There is no difference between coastal ( $n = 49$ , defined as within 1km of the coast) and  
 386 'inland' locations ( $n = 39$ ), as far as the latter can be said to exist on the small, low-lying  
 387 islands of the archipelago (Student's  $t$ -test,  $t = 1.14$ ,  $p = 0.26$ ,  $df = 86$ ).

388 6) No differences are seen between the four recorded Bahamian soil types (Bahamas Black  
 389 Loam, Bahamas Red Loam, Coral Sand and Brackish Swamp), which are all identical to five  
 390 decimals with the overall average of  $0.70917$  (ANOVA,  $F = 0.42$ ,  $p = 0.74$ ,  $df = 3, 31$ ). Two

samples from Middle Caicos (M7 and M12 in Table 1), noted in the field as growing on reddish/yellow-brown soils have ratios of 0.709169 and 0.709165, respectively at and slightly below the average both for Middle Caicos, and for all islands combined.

## DISCUSSION

The  $^{87}\text{Sr}/^{86}\text{Sr}$  taken up by trees across the Bahamas and TCI is consistent with an entirely autochthonous origin. A caveat here is the expected contribution of Sr in sea-spray, which affects the  $^{87}\text{Sr}/^{86}\text{Sr}$  ratios of both soils and plants along the coasts of many Caribbean islands (Bataille et al., 2012; Laffoon et al., 2012; Pestle et al., 2013). But this will not be detectable in the Bahamian archipelago, since the value for sea-spray will be indistinguishable from that of the islands' late Quaternary limestone bedrock (cf. Borg and Banner 1996). Furthermore, in Sr-rich carbonate formations (ca. 610 ppm), seawater (7-8 ppm) is not expected to be a significant factor (Faure, 1986; Angino et al., 1996; Borg and Banner, 1996; see also Snoeck, 2014). Rainfall is more complicated, since in the summer months it will contain Saharan dust particles, and so have a combination of Sr from both seawater and dust sources, though the concentration of Sr in precipitation is orders of magnitude less than in seawater ( $<0.1$  ppm; Faure, 1986; Capo et al., 1998) apart from its dust nuclei (200-300 ppm; Grousset et al., 1992; Rognon et al., 1996; Grousset and Biscaye, 2005). Therefore, precipitation on its own will not be a significant contributor of Sr.

More noteworthy for the present discussion is the absence of evidence for any measureable input in the overall dataset from atmospheric dust sources with different  $^{87}\text{Sr}/^{86}\text{Sr}$  ratios, whether lower ratios from volcanic ashfalls (ca. 0.707), or higher ratios from Saharan dust (ca. 0.716–0.718) (Grousset et al., 1992; Kroma et al., 1999; Grousset and Biscaye, 2005;

Formenti et al., 2011; Aarons et al., 2013). Even if present in only small amounts, either should have a discernable impact on the observed ratio for modern trees of 0.70917. For example, using a value of 0.71788 for Saharan dust (Bataille et al., 2012:7), a contribution of only 0.5% would raise the  $^{87}\text{Sr}/^{86}\text{Sr}$  ratio by over four standard deviations above the average of 0.70917 obtained for trees growing in the Bahamas/TCI in this project.

As might be expected given the striking homogeneity of our dataset, no convincing evidence could be found for even slight effects of Saharan dust or volcanic ashfalls on islands with greater summer dust-carrying rainfall, in 'inland' versus coastal locations, in different topographic positions, or on different soils, including a small number growing on lateritic 'red soils' (Figure 5). The only statistically significant difference that was observed relates to the greater variability in  $^{87}\text{Sr}/^{86}\text{Sr}$  ratios on TCI compare to the Bahamas. While it is conceivable that a small amount of volcanic ashfall is responsible for the lower ratios, we find this improbable based on previous studies addressing this issue (Muhs et al., 2007). Alternatively, it may be that these particular trees were growing on soils derived in part from middle Pleistocene deposits with lower  $^{87}\text{Sr}/^{86}\text{Sr}$  ratios (Hodell et al., 1990; Kindler et al., 2011). Unfortunately, as noted above, we have no detailed geological maps for TCI and thus are unable at present to address this matter further. Furthermore, detailed surficial geological mapping on the Bahamas, and by extension TCI, is extremely difficult due to the spatial patchiness of original deposition and subsequent uneven erosion (Carew and Mylroie, 1992). At the upper end of the  $^{87}\text{Sr}/^{86}\text{Sr}$  range, there are only two samples more than two standard deviations above the mean, which is in keeping with what would be expected from measurement error alone given our sample size. There is no need, therefore, to invoke any impact of Saharan dust to explain these outliers.

The results reported here for 91 modern trees fall well outside the predicted range of  $^{87}\text{Sr}/^{86}\text{Sr}$  ratios (0.70937 - 0.71030) for the Bahamas and Turks and Caicos Islands from Bataille et al. (2012; Fig. 5B, raster dataset available from [waterisotopes.org](http://waterisotopes.org), Bowen, 2017) (Figures 7 and 8). The predicted values are based on a three-source mixing model, which takes into account weighted inputs from bedrock weathering, atmospheric mineral dust, and sea salt. Whilst the weighting of the inputs varies spatially, the  $^{87}\text{Sr}/^{86}\text{Sr}$  ratios for bedrock (0.7080 – Bataille and Bowen, 2012), mineral dust (0.71788 – the mean of mineral dust collected over the Caribbean region from Grousset and Biscaye, 2005 and Formenti et al., 2011) and sea salt (0.7092 – the mean of bulk seawater) are constant. The value of 0.7080 used for bedrock in the model is based on the U.S. Geological Survey map of the Caribbean region (French and Schenk, 2004), which characterizes the surface geology of the Bahamas and Turks and Caicos Islands as ‘Quaternary alluvium’, and is given this ratio using the analogous descriptor from Bataille and Bowen (2012). However, this ratio is inappropriate for the islands’ late Quaternary marine carbonate bedrock with a value to four decimals of 0.7092.

Given the erroneously low  $^{87}\text{Sr}/^{86}\text{Sr}$  ratio of bedrock and the equivalence of ratios for sea salt and plant samples in the present study, the model significantly overestimates the input of mineral dust. The potential sources of error in the predicted Sr isoscape for the circum-Caribbean region, not least those resulting from the resolution of the surface geology database and the uncertainties of modeling aerosol deposition, are acknowledged by Bataille et al. (2012), who were exploring large-scale regional patterning and so were primarily interested in modeling broad trends. No  $^{87}\text{Sr}/^{86}\text{Sr}$  measurements were available for the Bahamas and Turks and Caicos Islands to validate their model at the time. Even at the broad scale at which it is intended to apply, the measured ratios for plant samples in

the present study indicate that the model is a poor fit for the Bahamian archipelago. That the predicted range of 0.709–0.710 actually encompasses our observed value of 0.70917 is fortuitous given the use of an inappropriate bedrock value of 0.7080. Substituting a more accurate  $^{87}\text{Sr}/^{86}\text{Sr}$  bedrock ratio of 0.7092 would have resulted in even higher predicted ratios for our study area, far above what was observed.

The recent publication of a Sr isoscape for Trinidad and Tobago, again based on measurements of modern trees (Ostapkowicz et al., 2017: Fig. 11), provides an additional test of the predictions made in Bataille et al.'s (2012; cf. Laffoon et al., 2016) model. We focus here on Tobago, since it has a simpler geology, being part of a Cretaceous volcanic arc, with a zone of Pleistocene marine deposits confined to the south of the island (Frost and Snoke, 1989; French and Schenk, 2004). Moreover, the bedrock  $^{87}\text{Sr}/^{86}\text{Sr}$  values for the volcanic arc are low ( $0.7038 \pm 0.0005$ ;  $n = 18$ ) (data from Frost and Snoke, 1989: Tab. 3), so that any influence of Saharan dust should be readily apparent. In this case there does appear to be a significant impact from marine sources (sea-spray and precipitation) and/or Saharan dust (bioavailable  $^{87}\text{Sr}/^{86}\text{Sr}$  excluding the limestone region:  $0.7058 \pm 0.0010$ ,  $n = 17$ ; data from Ostapkowicz et al., 2017: Tab. 3). The predicted ratios of between 0.7049 and 0.7096 for Tobago in Ostapkowicz et al.'s (2017) new isoscape (with the high end of this range confined to the Pleistocene marine deposits of the southwest end of the island) are at the lower end of the range predicted by Bataille et al.'s model (0.7038 to 0.7129, with the low values restricted to a very small part of the island) (2012; Fig. 5B, raster dataset available from [waterisotopes.org](https://waterisotopes.org), Bowen, 2017) (Figure 9). This is particularly noteworthy in that the bedrock geology across most of Tobago is much more resistant to weathering than marine carbonates, and so a correspondingly greater contribution from allochthonous sources would be expected (Bataille et al., 2012: Fig. 6B).

491  
492   Accepting that Saharan dust contributes significantly to the soils of the Bahamas/TCI, why  
493   do we not see any impact on strontium isotope ratios in the biosphere? Bataille et al.  
494   (2012) emphasize the importance of taking airborne mineral dust into account, but note  
495   that its contribution is variable across the circum-Caribbean, decreasing from east to west,  
496   and is also dependent on the bedrock substrate of the island in question, in relation to both  
497   its susceptibility to erosion and the amount of Sr it contains. While the marine carbonates  
498   of the Antilles and the Bahamian archipelago can be characterized as highly weatherable,  
499   they leave little material behind when they enter solution, and simply wash away (Borg  
500   and Banner, 1996). This is why researchers emphasize the difficulty of developing soils on  
501   limestone islands, since they contain relatively few other minerals besides  $\text{CaCO}_3$ . However,  
502   they are Sr-rich, and so will contribute in an ongoing fashion to the pool of biologically  
503   available Sr on the islands.

504  
505   Central to the discussion is not only the relative Sr concentrations in limestone and in  
506   Saharan dust, and their respective  $^{87}\text{Sr}/^{86}\text{Sr}$  ratios, but also the bioavailability of Sr. As  
507   already noted, the  $^{87}\text{Sr}/^{86}\text{Sr}$  value of late Quaternary deposits in the Bahamian archipelago  
508   is tightly constrained to  $\sim 0.7092$ . Carbonates have some of the highest Sr concentrations  
509   found in rock, on the order of 610 ppm (Faure, 1986; Capo et al., 1998). The Sr  
510   concentration of Saharan dust has been variously reported as being from one-half (286  
511    $\pm 58$  ppm; Grousset et al., 1992) to one-third of this (195 ppm; Rognon et al., 1996;  
512   Grousset and Biscaye, 2005). The more recent latter figure is used in Bataille et al.'s  
513   (2012:7) isoscape model. Saharan dust is highly radiogenic in a Caribbean context, with an  
514    $^{87}\text{Sr}/^{86}\text{Sr}$  value of ca. 0.71788 (Grousset and Biscaye, 1989; 2005; Grousset et al., 1992;  
515   Formenti et al., 2011). However, this refers to the bulk measurement of airborne dust

particles, much of which (>70%) will take the form of the clay minerals mica-illite and kaolinite with decreasing amounts of quartz with distance from the source (Glaccum and Prospero, 1980; see also Caquineau et al., 2002). Strontium associated with mica and especially quartz will not be readily bioavailable due to the relatively low solubility of these minerals (Rummel et al., 2010:892). Concentrations of highly soluble calcite, on the other hand, were found to be a minor component at consistently less than 10% (Glaccum and Prospero, 1980). Aarons et al. (2013: Fig. 2) separated the soluble and insoluble fractions for  $^{87}\text{Sr}/^{86}\text{Sr}$  measurements of Saharan dust collected in a North Atlantic transect. They found that the soluble fraction was invariably less radiogenic (0.7108) than the insoluble silicate fraction (0.7159), attributing this to the former's dilution with sea-salt, unsurprising given the use of shipboard collection filters. The point to be made here is that the dust included strontium in its insoluble fraction, which would not be readily bioavailable.

Thus, the bioavailability of Sr in Saharan dust is unclear. As noted above,  $\text{Sr}^{2+}$  will be adsorbed onto negatively charged clay minerals and organic matter (Capo et al., 1998). In this sense Sr would be held in the soil, but once adsorbed it would need to desorb as part of the soil exchange process before becoming available to be taken up by plant roots. Studies have shown that both clay and organic matter inhibit the transfer of soil Sr to plants (Baes et al., 1986; Lembrechts, 1993). Other complicating factors include the presence of competing ions in the soil (e.g.,  $\text{Na}^{2+}$ ), the concentration ratio of Sr to other micro- and macro-nutrients, and microenvironments (including ion depletion) created in the rooting zone by the plants themselves, all of which combine to render the concept of 'bioavailability' difficult to operationalize within a given context (Ehlken and Kirchner,

2002). To this can be added the relationship between the timing of dustfall and the growing season.

The empirical results presented in this paper differ substantially from the predictions made by the current Sr isotope model for the Caribbean, which, while noting the dominance of bedrock weathering to the bioavailable Sr flux in carbonate regions such as those of the Bahamian archipelago, nevertheless still predicts a 20-30% contribution of atmospheric dust sources in the southern archipelago, decreasing to 10-20% in the north (Bataille et al., 2012: Fig. 5A). Our results suggest that the contribution of airborne dust to the Sr flux is considerably lower than this, and is in fact undetectable in a comparatively large sample of 91 measurements. However, it is still necessary to sample a greater range of terrestrial vegetation than we have done here, including grasses, before concluding that there is absolutely no effect on the islands' biosphere, with the further implication of little to no impact of Saharan dust on  $^{87}\text{Sr}/^{86}\text{Sr}$  ratios in the biosphere in other carbonate regions of the Caribbean, including Florida.

## CONCLUSIONS

Our results suggest that Saharan dust does not make a significant contribution to bioavailable Sr in the Bahamian archipelago, and that bedrock is the main driver. The contribution of sea-spray is not detectable isotopically because of the near-equivalence of modern ocean and late Quaternary carbonate  $^{87}\text{Sr}/^{86}\text{Sr}$  ratios, though the much higher Sr concentration of the latter means that this source will be overwhelmingly dominant in any case. Our results support the proposition that highly weatherable carbonate bedrock will override the influence of North African dust, though the full extent of this was previously



not clear. For the 91 trees in our study we found over an order of magnitude less influence of Saharan dust than predicted by Bataille et al.'s (2012) Sr isoscape. Similarly, a Sr isoscape recently created for Trinidad and Tobago (Ostapkowicz et al., 2017) suggests a lower contribution of Saharan dust to Tobago's biosphere than predicted by Bataille et al.'s model.

The impact of Saharan dust on bioavailable  $^{87}\text{Sr}/^{86}\text{Sr}$  ratios in the Caribbean and elsewhere needs to be revisited, potentially reducing its significance for ecological and archaeological provenience studies in the biosphere and underlining the need to tailor isoscapes to individual contexts (cf. Wunder 2010:251-252). The extent to which the findings in the present study apply to other parts of the circum-Caribbean region and further afield would benefit from further investigation. Even within the Bahamian archipelago, a study focused more specifically on the 'red soils' is needed, in order to determine the extent to which these soils can be distinguished isotopically from the other soils of the islands. Similarly, the impact of seawater as an allochthonous input would be more appropriately investigated by targeting vegetation growing on the limited exposures of early and middle Pleistocene deposits. We intend to address these matters in the future.

## ACKNOWLEDGEMENTS

This research was supported by a grant from the Getty Foundation and by the Max Planck Institute. Many thanks to Annabell Reiner and Sven Steinbrenner for assistance with strontium isotope preparation and measurement, to Richard Cant and Sherriley Strachan, Chief Archivist of the National Archives of the Bahamas, for providing access to materials relating to the soils of the Bahamas, and to Claire Sedgwick, Registrar, World Museum,

Liverpool, for help with CITES documentation. Thanks also to Gabe Bowen for repairing the links to the strontium dataset for the Caribbean used in Bataille et al. (2012). We are grateful for the detailed comments made by Brooke Crowley and an anonymous reviewer as well as by the journal's editor, which have greatly improved the clarity and focus of the paper.

## REFERENCES

Aarons, S.M., Aciego, S.M., Gleason, J.D., 2013. Variable Hf–Sr–Nd radiogenic isotopic compositions in a Saharan dust storm over the Atlantic: Implications for dust flux to oceans, ice sheets and the terrestrial biosphere. *Chemical Geology* 349–350, 18–26.

Åberg, G., Jacks, G., Wickman, T., Hamilton, P.J., 1990. Strontium isotopes in trees as an indicator for calcium availability. *Catena* 17, 1–11.

Angino, E.E., Billings, G.K., Andersen, N., 1996. Observed variations in the strontium concentration of sea water. *Chemical Geology* 1, 145–153.

Baes, C.F., Garten, C.T., Taylor, F.G., Witherspoon, J.P., 1986. Long-term environmental problems of radioactively contaminated land. *Environment International* 12(5), 543–553.

Bain, D.C., Bacon, J.R., 1994. Strontium isotopes as indicators of mineral weathering in catchments. *Catena* 22, 201–214.

Bataille, C.P., Bowen, G.J., 2012. Mapping  $^{87}\text{Sr}/^{86}\text{Sr}$  variations in bedrock and water for large scale provenance studies. *Chemical Geology* 304–305, 39–52.

615

616 Bataille, C.P., Laffoon, J., Bowen, G.J., 2012. Mapping multiple source effects on the  
617 strontium isotopic signatures of ecosystems from the Circum-Caribbean region. *Ecosphere*  
618 3, 118.

619

620 Bern, C.R., Townsend, A.R., Farmer, G.L., 2005. Unexpected dominance of parent-material  
621 strontium in a tropical forest on highly weathered soils. *Ecology* 86, 626–632.

622

623 Boardman, M.R., McCartney, R.F., Eaton, M.R., 1995. Bahamian paleosols: origin, relation to  
624 paleoclimate, and stratigraphic significance. In: Curran, H.A., White, B. (Eds.), *Terrestrial*  
625 *and Shallow Marine Geology of the Bahamas and Bermuda*, Geological Society of America  
626 Special Paper, vol. 300, pp. 33–49.

627

628 Borg, L.E., Banner, J.L., 1996. Neodymium and strontium isotopic constraints on soil  
629 sources in Barbados, West Indies. *Geochimica et Cosmochimica Acta* 60, 4193–4206.

630

631 Bowen, G.J., 2017. Gridded maps of the isotopic composition of meteoric waters.  
632 <http://www.waterisotopes.org>.

633

634 Bricker, O., Mackenzie, F.T., 1970. Limestones and red soils of Bermuda: discussion.  
635 *Geological Society of America Bulletin* 81, 2523–2524.

636

637 Capo, R.C., DePaolo, D.J., 1990. Seawater strontium isotopic variations from 2.5 million  
638 years ago to the present. *Science* 249: 51–55.

639

640 Capo, R.C., Stewart, B.W., Chadwick, O.A., 1998. Strontium isotopes as tracers of ecosystem  
641 processes: theory and methods. *Geoderma* 82, 197-225.

642

643 Caquineau, S., Gaudichet, A., Gomes, L., Legrand, M., 2002. Mineralogy of Saharan dust  
644 transported over northwestern tropical Atlantic Ocean in relation to source regions.  
645 *Journal of Geophysical Research, Atmospheres* 107, AAC 4-1–AAC 4-12.

646

647 Carew, J.L., Mylroie, J.E., 1985. The Pleistocene and Holocene stratigraphy of San Salvador  
648 Island, Bahamas, with reference to marine and terrestrial lithofacies at French Bay. In:  
649 Curran, H.A. (Ed.), *Pleistocene and Holocene Carbonate Environments on San Salvador*  
650 *Island, Bahamas, Ft. Lauderdale, CCFL Bahamian Field Station*, pp. 11-61.

651

652 Carew, J.L., Mylroie, J.E., 1995. Depositional model and stratigraphy for the Quaternary  
653 geology of the Bahama Islands. In: Curran, H.A., White, B. (Eds.), *Terrestrial and Shallow*  
654 *Marine Geology of the Bahamas and Bermuda, Boulder, Geological Society of America*  
655 *Special Paper*, 300, pp. 5-32.

656

657 Carew, J.L., Mylroie, J.E., 1997. Geology of the Bahamas. In: Vacher, H.L., Quinn, T. (Eds.),  
658 *Geology and Hydrogeology of Carbonate Islands*, Elsevier, Amsterdam, pp. 91-139.

659

660 Chen, J.H., Curran, H.A., White, B., Wasserburg, G.J., 1991. Precise chronology of the last  
661 interglacial period:  $^{234}\text{U}$ - $^{230}\text{Th}$  data from fossil coral reefs in the Bahamas. *Geological*  
662 *Society of America Bulletin* 103(1), 82-97.

663

664 Colarco, P.R., Toon, O.B., Holben, B.N., 2003. Saharan dust transport to the Caribbean during

665 PRIDE: 1. Influence of dust sources and removal mechanisms on the timing and magnitude  
 666 of downwind aerosol optical depth events from simulations of in situ and remote sensing  
 667 observations. *Journal of Geophysical Research–Atmospheres* 108.

668

669 Copeland, S.R., Sponheimer, M., le Roux, P.J., Grimes, V., Lee-Thorp, J.A., de Ruiter, D.J.,  
 670 Richards, M.P., 2008. Strontium isotope ratios ( $^{87}\text{Sr}/^{86}\text{Sr}$ ) of tooth enamel: a comparison of  
 671 solution and laser ablation multicollector inductively coupled plasma mass spectrometry  
 672 methods. *Rapid Communications in Mass Spectrometry* 22, 3187-3194.

673

674 Correll, D.S., Correll, B., 1982. *Flora of the Bahama Archipelago, including the Turks and*  
 675 *Caicos Islands*, Vaduz, A. R. Gantner Verlag.

676

677 Delany, A.C., Parkin, D.W., Griffin, J.J., Goldberg, E.D., Reimann, B.E.F., 1967. Airborne dust  
 678 collected at Barbados. *Geochemica et Cosmochemica Acta* 31, 885-909.

679

680 Dia, A.N., Cohen, A.S., Onions, R.K., Shackleton, N.J., 1992. Seawater Sr isotope variation over  
 681 the past 300Kyr and influence of global climate cycles. *Nature* 356, 786–788.

682

683 Ehlken, S., Kirchner, G., 2002. Environmental processes affecting plant root uptake of  
 684 radioactive trace elements and variability of transfer factor data: a review. *Journal of*  
 685 *Environmental Radioactivity* 58(2-3), 97-112.

686

687 Evans, J.A., Montgomery, J., Wildman, G., Boulton, N., 2010. Spatial variations in biosphere  
 688  $^{87}\text{Sr}/^{86}\text{Sr}$  in Britain. *Journal of the Geological Society, London* 167, 1-4.

689

690 Faure, G., 1986. Principles of Isotope Geology. John Wiley, New York.

691

692 Fick, S.E., Hijmans, R.J., 2017. WorldClim 2: new 1-km spatial resolution climate surfaces for  
693 global land areas. International Journal of Climatology 37.

694

695 Foos, A.M., 1991. Aluminous lateritic soils, Eleuthera, Bahamas: a modern analogue to  
696 carbonate paleosols. Journal of Sedimentary Petrology 61, 340-348.

697

698 Foos, A.M., Bain, R.J., 1995. Mineralogy, chemistry, and petrography of soils, surface crusts,  
699 and soil stones, San Salvador and Eleuthera, Bahamas. In: Curran, H.A., White, B. (Eds.),  
700 Terrestrial and Shallow Marine Geology of the Bahamas and Bermuda, Geological Society  
701 of America Special Paper, 300, pp. 223-232.

702

703 Formenti, P., Schutz, L., Balkanski, Y., Desboeufs, K., Ebert, M., Kandler, K., Petzold, A.,  
704 Scheuven, D., Weinbruch, S., Zhang, D., 2011. Recent progress in understanding physical  
705 and chemical properties of African and Asian mineral dust. Atmospheric Chemistry and  
706 Physics 11, 8231-8256.

707

708 French, C.D., Schenk, C.J., 2004. Map Showing Geology, Oil and Gas Fields, and Geologic  
709 Provinces of the Caribbean Region, Geological Survey, Open-File Report 97-470-K, Central  
710 Energy Resources Team, Denver.

711

712 Frost, C.D., Snoke, A.W., 1989. Tobago, West Indies, a fragment of a Mesozoic oceanic island  
713 arc: petro-chemical evidence. Journal of the Geological Society 146, 953-964.

714

715 Glaccum, R.A., Prospero, J.M., 1980. Saharan aerosols over the tropical North Atlantic—  
 716 mineralogy. *Marine Geology* 37, 295–321.  
 717

718 Gosz, J.R., Moore, D.I., 1989. Strontium isotope studies of atmospheric inputs to forested  
 719 watersheds in New Mexico. *Biogeochemistry* 8, 115-134.  
 720

721 Graustein, W.C., Armstrong, R.L., 1983. The use of strontium-87/strontium-86 ratios to  
 722 measure transport into forested watersheds. *Science* 219, 289-292.  
 723

724 Grousset, F.E., Biscaye, P.E., 1989. Nd and Sr isotopes as tracers of wind transport: Atlantic  
 725 aerosols and surface sediments. In: Leinen, M., Sarnthein, M. (Eds.), *Paleoclimatology and*  
 726 *Paleometeorology: Modern and Past Patterns of Global Atmospheric Transport*, Kluwer  
 727 Academic, Amsterdam, pp. 385-400.  
 728

729 Grousset, F.E., Biscaye, P.E., 2005. Tracing dust sources and transport patterns using Sr, Nd  
 730 and Pb isotopes. *Chemical Geology* 222, 149–167.  
 731

732 Grousset, F.E., Rognon, P., Coudé-Gaussen, G., Pédemay, P., 1992. Origins of peri-Saharan  
 733 dust deposits traced by their Nd and Sr isotopic composition. *Palaeogeography,*  
 734 *Palaeoclimatology, Palaeoecology* 93, 203-212.  
 735

736 Hartman, G., Richards, M., 2014. Mapping and defining sources of variability in bioavailable  
 737 strontium isotope ratios in the Eastern Mediterranean. *Geochimica et Cosmochimica Acta*  
 738 126, 250-254.  
 739

740 Hearty, P.J., 1998. The geology of Eleuthera Island, Bahamas: A rosetta stone of Quaternary  
741 stratigraphy and sea-level history. *Quaternary Science Reviews* 17, 333-355.  
742

743 Hearty, P.J., Kindler, P., 1993. New perspectives on Bahamian geology: San Salvador Island,  
744 Bahamas. *Journal of Coastal Research* 9(2), 577-594.  
745

746 Hearty, P.J., Kindler, P., 1997. The stratigraphy and surficial geology of New Providence and  
747 surrounding islands, Bahamas. *Journal of Coastal Research* 13(3), 798-812.  
748

749 Henderson, G.M., Martel, D.J., O’Nions, R.K., Shackleton, N.J., 1994. Evolution of seawater  
750  $^{87}\text{Sr}/^{86}\text{Sr}$  over the last 400 ka: the absence of glacial/interglacial cycles. *Earth and Planetary*  
751 *Science Letters* 128, 643-651.  
752

753 Herwitz, S.R., Muhs, D.R., Prospero, J.M. and Vaughn, B. 1996. Origins of Bermuda's clay-rich  
754 paleosols and their climatic significance. *Journal of Geophysical Research-Atmospheres*  
755 101, 23389-23400.  
756

757 Hodell, D.A., Mead, G.A., Mueller, P.A., 1990. Variation in the strontium isotopic composition  
758 of seawater (8 Ma to present): Implications for chemical weathering rates and dissolved  
759 fluxes to the oceans. *Chemical Geology: Isotope Geoscience Section* 80, 291-307.  
760

761 Hodell, D.A., Quinn, R.L., Brenner, M., Kamenov, G., 2004. Spatial variation of strontium  
762 isotopes ( $^{87}\text{Sr}/^{86}\text{Sr}$ ) in the Maya region: a tool for tracking ancient human migration.  
763 *Journal of Archaeological Science* 31(5), 585-601.  
764



765 Kamenov, G.D., Brenner, M., Tucker, J.L., 2009. Anthropogenic versus natural control on  
766 trace element and Sr–Nd–Pb isotope stratigraphy in peat sediments of southeast Florida  
767 (USA), ~1500 AD to present. *Geochimica et Cosmochimica Acta* 73, 3549–3567.  
768

769 Kaufman, Y.J., Koren, I., Remer, L.A., Tanré, D., Ginoux, P., Fan, S., 2005. Dust transport and  
770 deposition observed from the Terra-Moderate Resolution Imaging Spectroradiometer  
771 (MODIS) spacecraft over the Atlantic Ocean. *Journal of Geophysical Research* 119, D10S12.  
772

773 Kennedy, M.J., Chadwick, O.A., Vitousek, P.M., Derry, L.A., Hendricks, D.M., 1998. Changing  
774 sources of base cations during ecosystem development, Hawaiian Islands. *Geology* 26,  
775 1015–1018.  
776

777 Kindler, P., Godefroid, F., Chiaradia, M., Ehlert, C., Eisenhauer, A., Frank, M., Hasler, C.-A.,  
778 Samankassou, E., 2011. Discovery of Miocene to early Pleistocene deposits of Mayaguana,  
779 Bahamas. *Geology* 39, 986-979.  
780

781 Kroma, M.D., Cliff, R.A., Eijssink, L.M., Herut, B., Chester, R., 1999. The characterisation of  
782 Saharan dusts and Nile particulate matter in surface sediments from the Levantine basin  
783 using Sr isotopes. *Marine Geology* 155, 319–330.  
784

785 Kuznetsov, A.B., Semikhatov, M.A., Gorokhov, I.M., 2012. The Sr isotope composition of the  
786 world ocean, marginal and inland seas: Implications for the Sr isotope stratigraphy.  
787 *Stratigraphy and Geological Correlation* 20(6), 501–515.  
788

789 Laffoon, J.E., Davies, G.R., Hoogland, M.L.P., Hofman, C.L., 2012. Spatial variation of

790 biologically available strontium isotopes ( $^{87}\text{Sr}/^{86}\text{Sr}$ ) in an archipelagic setting: a case  
 791 study from the Caribbean. *Journal of Archaeological Science* 39, 2371-2384.  
 792

793 Laffoon, J.E., Hoogland, M.L.P., 2012. Migration and mobility in the circum-Caribbean:  
 794 Integrating archaeology and isotopic analysis. In: Kaiser, E., Burger, J., Schier, W. (Eds.),  
 795 Population Dynamics in Prehistory and Early History: New Approaches Using Stable  
 796 Isotopes and Genetics, Amsterdam, de Gruyter, pp. 337-353.  
 797

798 Laffoon, J.E., Rodríguez Ramos, R., Chanlatte Baik, L., Storde, Y.N., Rodríguez Lopez, M.,  
 799 Davies, G.R., Hofman, C.L., 2014. Long-distance exchange in the precolonial Circum-  
 800 Caribbean: A multi-isotope study of animal tooth pendants from Puerto Rico. *Journal of*  
 801 *Anthropological Archaeology* 35, 220-233.  
 802

803 Laffoon, J.E., Sonnemann, T.F., Antczak, M.M., Antczak, A., 2016. Sourcing nonnative  
 804 mammal remains from Dos Mosquises Island, Venezuela: new multiple isotope evidence.  
 805 *Archaeological and Anthropological Sciences*, doi: 10.1007/s12520-016-0453-6.  
 806

807 Laffoon, J.E., Sonnemann, T.F., Shafie, T., Hofman, C.L., Brandes, U., Davies, G.R., 2017.  
 808 Investigating human geographic origins using dual-isotope ( $^{87}\text{Sr}/^{86}\text{Sr}$ ,  $\delta^{18}\text{O}$ ) assignment  
 809 approaches. *PLoS ONE* 12(2), e0172562.  
 810

811 Lehnert, K., Su, Y., Langmuir, C.H., Sarbas, B., Nohl, U., 2000. A global geochemical database  
 812 structure for rocks. *Geochemistry Geophysics Geosystems* 1. doi: 10.1029/1999GC000026  
 813

814 Lembrechts, J., 1993. A review of literature on the effectiveness of chemical amendments in

815    reducing the soil-to-plant transfer of radiostrontium and radiocesium. *Science of the Total*  
816    *Environment* 137(1-3), 81-98.

817

818    Little, B.G., Buckley, D.K., Cant, R., Henry, P.W.T., Jefferies, A., Mather, J.D., Stark, J., Young,  
819    R.N., 1977. The Land Resources of the Bahamas: A Summary. Land Resources Division,  
820    Ministry of Overseas Development, Study 27.

821

822    Lovett, G.M., Lindberg, S.E., 1984. Dry deposition and canopy exchange in a mixed oak  
823    forest as determined by analysis of throughfall. *Journal of Applied Ecology* 21, 1013-1027.

824

825    McArthur, J.M., 1994. Recent trends in strontium isotope stratigraphy. *Terra Nova* 6, 331-  
826    358.

827

828    Montgomery, J., Evans, J.A., Neighbour, T., 2003. Sr isotope evidence for population  
829    movement within the Hebridean Norse community of NW Scotland. *Journal of the*  
830    *Geological Society, London* 160, 649-653.

831

832    Mooney, C.N., 1905. Soils of the Bahama Islands. In: Shattuck, G.B. (Ed.), *The Bahama*  
833    *Islands*, Macmillan, New York, pp. 147-184.

834

835    Muhs, D.R., Budahn, J.R., Prospero, J.M., Carey, S.N., 2007. Geochemical evidence for African  
836    dust inputs to soils of western Atlantic islands: Barbados, the Bahamas, and Florida. *Journal*  
837    *of Geophysical Research: Earth Surface*, 112. doi: 10.1029/2005JF000445.

838

839    Muhs, D.R., Bush, C.A., Stewart, K.C., Rowland, T.R., Crittenden, R.C., 1990. Geochemical

840 evidence of Saharan dust parent material for soils developed on Quaternary limestones of  
841 Caribbean and Western Atlantic islands. *Quaternary Research* 33, 157-177.

842

843 Muhs, D.R., Crittenden, R.C., Rosholt, J.N., Bush, C.A., Stewart, K.C., 1987. Genesis of marine  
844 terrace soils, Barbados, West Indies: Evidence from mineralogy and geochemistry. *Earth*  
845 *Surface Processes and Landforms* 12, 605-618.

846

847 Mylroie, J.E., Carew, J.L., 1995. Geology and karst geomorphology of San Salvador Island,  
848 Bahamas. *Carbonates and Evaporites* 10(2), 193–206.

849

850 Nowotnick, E., Colarco, P., da Silva, A., Hlavka, D., McGill, M., 2011. The fate of Saharan dust  
851 across the Atlantic and implications for a Central American dust barrier. *Atmospheric*  
852 *Chemistry and Physics* 11, 8415-8431.

853

854 Ostapkowicz, J., 2015. Either a piece of domestic furniture of the Indians or one of their  
855 Gods': the study of Lucayan duhos. *Journal of Caribbean Archaeology* 15, 62-66.

856

857 Ostapkowicz, J., Brock, F., Wiedenhoef, A., Snoeck, C., Pouncett, J., Baksh-Comeau, Y.,  
858 Schulting, R., Boomert, A., 2017. Black pitch, carved histories: AMS <sup>14</sup>C, wood ID and  
859 strontium results on prehistoric wood carvings from Trinidad's Pitch Lake. *Journal of*  
860 *Archaeological Science: Reports* 16, 341-358.

861

862 Ostapkowicz, J., Bronk Ramsey, C., Brock, F., Cartwright, C.R., Stacey, R., Richards, M., 2013.  
863 Birdmen, cemís and duhos: material studies and AMS <sup>14</sup>C dating of Pre-Hispanic Caribbean  
864 wood sculptures in the British Museum. *Journal of Archaeological Science* 40, 4675-4687.

865

866 Ostapkowicz, J., Naqqi Manco, B., Richards, M., Wiedenhoeft, A., 2012. Hidden Stories: Trees  
867 and the charting of Lucayan histories. *Times of the Islands*, Summer, 22-27.

868

869 Pestle, W.J., Simonetti, A., Curet, L.A., 2013.  $^{87}\text{Sr}/^{86}\text{Sr}$  variability in Puerto Rico: geological  
870 complexity and the study of paleomobility. *Journal of Archaeological Science* 40, 2561-  
871 2569.

872

873 Poszwa, A., Dambrine, E., Ferry, B., Pollier, B., Loubet, M., 2002. Do deep tree roots provide  
874 nutrients to the tropical rainforest? *Biogeochemistry* 60, 97-118.

875

876 Prognon, F., Cojan, I., Kindler, P., Thiry, M., Demange, M., 2011. Mineralogical evidence for a  
877 local volcanic origin of the parent material of Bermuda Quaternary paleosols. *Quaternary*  
878 *Research* 75, 256-266.

879

880 Prospero, J.M., 1999. Long-range transport of mineral dust in the global atmosphere:  
881 Impact of African dust on the environment of the southeastern United States. *Proceedings*  
882 *of the National Academy of Sciences (USA)* 96, 3396-3403.

883

884 Prospero, J.M., Carlson, T.N., 1972. Vertical and areal distribution of Saharan dust over  
885 western equatorial North-Atlantic Ocean. *Journal of Geophysical Research-Atmospheres*  
886 77, 5255-5260.

887

888 Prospero, J.M., Glaccum, R.A., Nees, R.T., 1981. Atmospheric transport of soil dust from  
889 Africa to South America. *Nature* 289, 570-572.

890

891 Prospero, J.M., Lamb, P.J., 2003. African droughts and dust transport to the Caribbean:  
 892 climate change implications. *Science* 302, 1024– 1027.

893

894 Prospero, J.M., Mayol-Bracero, O.L., 2013. Understanding the transport and impact of  
 895 African dust on the Caribbean basin. *Bulletin of the American Meteorological Society* 94,  
 896 1329-1337.

897

898 Prospero, J.M., Nees, R.T., Uematsu, M., 1987. Deposition rate of particulate and dissolved  
 899 aluminum derived from Saharan dust in precipitation at Miami, Florida, *Journal of*  
 900 *Geophysical Research-Atmospheres* 92. 14723–14731.

901

902 Pushkar, P., Steuber, A.M., Tomblin, J.F., Julian, G.M., 1973. Strontium isotopic ratios in  
 903 volcanic rocks from St. Vincent and St. Lucia, Lesser Antilles. *Journal of Geophysical*  
 904 *Research-Oceans* 78(8), 1279-1287.

905

906 Reinhardt, E.G., Blenkinsop, J., Patterson, R.T., 1999. Assessment of a Sr isotope vital effect  
 907 ( $^{87}\text{Sr}/^{86}\text{Sr}$ ) in marine taxa from Lee Stocking Island, Bahamas. *Geo-Marine Letters* 18, 241-  
 908 246.

909

910 Reynolds, A.C., Betancourt, J.L., Quade, J., Patchett, P.J., Dean, J.S., Stein, J., 2005.  $^{87}\text{Sr}/^{86}\text{Sr}$   
 911 sourcing of ponderosa pine used in Anasazi great house construction at Chaco Canyon, New  
 912 Mexico. *Journal of Archaeological Science* 32, 1061-1075.

913

914 Reynolds, A.C., Quade, J., Betancourt, J.L., 2012. Strontium isotopes and nutrient sourcing in

915 a semi-arid woodland. *Geoderma* 189-190, 574–584.

916

917 Ridley, D.A., Heald, C.L., Prospero, J.M., 2014. What controls the recent changes in African  
 918 mineral dust aerosol across the Atlantic? *Atmospheric Chemistry and Physics* 14(11),  
 919 5735–5747.

920

921 Rognon, P., Coudé-Gaussen, G., Revel, M., Grousset, F.E., Pedemay, P., 1996. Holocene  
 922 Saharan dust deposition on the Cape Verde Islands: sedimentological and Nd-Sr isotopic  
 923 evidence. *Sedimentology* 43, 359–366.

924

925 Rummel, S., Hoelzl, S., Horn, P., Rossmann, A., Schlicht, C., 2010. The combination of stable  
 926 isotope abundance ratios of H, C, N and S with  $^{87}\text{Sr}/^{86}\text{Sr}$  for geographical origin assignment  
 927 of orange juices. *Food Chemistry* 118, 890–900.

928

929 Sears, W.H., Sullivan, S.O., 1978. Bahamas prehistory. *American Antiquity* 43, 3-25.  
 930  
 931

932 Sillen, A., Hall, G., Richardson, S., Armstrong, R., 1998.  $^{87}\text{Sr}/^{86}\text{Sr}$  ratios in modern and fossil  
 933 food-webs of the Sterkfontein Valley: implications for early hominid habitat preference -  
 934 clues from context. *Geochimica et Cosmochimica Acta* 62, 2463-2472.

935

936 Spitzer, M., Wildenhain, J., Rappsilber, J., Tyers, M., 2014. BoxPlotR: a web tool for  
 937 generation of box plots. *Nature Methods* 11, 121-122.

938

939 Snoeck, C., 2014. Impact of strontium sea spray effect on the isotopic ratio ( $^{87}\text{Sr}/^{86}\text{Sr}$ ) of  
 940 plants in coastal Ireland. *Quaternary Newsletter* 134, 37–39.

941

942 Snoeck, C., Pouncett, J., Ramsey, G., Meighan, I.G., Mattielli, N., Lee-Thorp, J.A., Schulting, R.J.,  
 943 2016. Mobility during the Neolithic and Bronze Age in Northern Ireland explored using  
 944 strontium isotope analysis of cremated human bone. *American Journal of Physical*  
 945 *Anthropology* 160, 397–413.

946

947 Syers, J.K., Jackson, M.L., Berkheiser, V.E., Clayton, R.N., Rex, R.W., 1969. Eolian sediment  
 948 influence on pedogenesis during the Quaternary. *Soil Science* 107, 421–427.

949

950 Vitousek, P.M., Kennedy, M.J., Derry, L.A., Chadwick, O.A., 1999. Weathering versus  
 951 atmospheric sources of strontium in ecosystems on young volcanic soils. *Oecologia* 121,  
 952 255-259.

953

954 Wanless, H.R., Dravis, J.J., Tedesco, L.P., Rossinsky, V. 1989. *Carbonate Environments and*  
 955 *Sequences of Caicos Platform, Field Trip Guidebook T374*. American Geophysical Union,  
 956 Washington, D.C.

957

958 Whipkey, C.E., Capo, R.C., Chadwick, O.A., Stewart, B.W., 2000. The importance of sea spray  
 959 to the cation budget of a coastal Hawaiian soil: a strontium isotope approach. *Chemical*  
 960 *Geology* 168, 37-48.

961

962 Whitaker, F.F. and Smart, P.L., 1997. Hydrogeology of the Bahamian archipelago. In: Vacher,  
 963 H.L., Quinn, T. (Eds.), *Geology and Hydrogeology of Carbonate Islands*, Elsevier,  
 964 Amsterdam, pp. 183-216.

965



966 Wood, J. 1996. The Geomorphological Characterisation of Digital Elevation Models. PhD  
967 thesis, University of Leicester. Available at: <https://lra.le.ac.uk/handle/2381/34503>.  
968  
969 Wood, J. 2009. The Landsurf Manual, version 1.0. [landserf.org](http://landserf.org). Available at:  
970 <http://www.staff.city.ac.uk/~jwo/landserf/landserf230/doc/landserfManual.pdf>.  
971  
972 Wunder, M., 2010. Using isoscapes to model probability surfaces for determining  
973 geographic origins. In: West, J., Bowen, G., Dawson, T., Tu, K. (Eds.), *Isoscapes:  
974 Understanding Movement, Pattern, and Process on Earth through Isotope Mapping*.  
975 Springer, Dordrecht, pp. 251–270.  
976  
977  
978

## Table and Figure captions

Table 1.  $^{87}\text{Sr}/^{86}\text{Sr}$  results and metadata for sampled modern trees from the Bahamas and TCI.

Table 2. Summary statistics for  $^{87}\text{Sr}/^{86}\text{Sr}$  results by island.

Figure 1. Map of the study region showing the locations of islands sampled in this study. Lee Stocking Island is also identified as providing  $^{87}\text{Sr}/^{86}\text{Sr}$  results for various reef and mangrove taxa (Reinhardt et al., 1999). Data sources: SRTM Void Filled elevation data courtesy of the U.S. Geology Survey and The GEBCO\_2014 Grid, version 20150318, [www.gebco.net](http://www.gebco.net).

Figure 2. Percentage of annual precipitation for: a) summer; and b) winter. Data sources: WorldClim Version 2 (Fick and Hijmans, 2017) and The GEBCO\_2014 Grid, version 20150318, [www.gebco.net](http://www.gebco.net).

Figure 3. The distribution of the main soils and sample locations for: a) Cat Island; and b) Long Island. Data sources: Soils of the Bahama Islands (Mooney, 1905) and The GEBCO\_2014 Grid, version 20150318, [www.gebco.net](http://www.gebco.net).

Figure 4. Caicos Islands, Turks and Caicos, showing sample locations. Sampling on North, Middle and East Caicos is concentrated along the north coasts due to the absence of trees on the swampland and tidal flats of the southern half of the islands. Data sources: The GEBCO\_2014 Grid, version 20150318, [www.gebco.net](http://www.gebco.net).

Figure 5a) small *Swietenia mahagoni* growing on flooded 'Bahama Black Loam', south of Old Bight, Cat Island (C7); b) medium *Swietenia mahagoni* growing on 'Coral Sand', Hamilton's, Long Island (L7); c) medium *Guaiacum sanctum* growing on yellow-brown loam, Lorimer's, Middle Caicos (M7); d) small *Guaiacum sanctum* bush growing on shallow 'Bahama Red Loam', south of Scrub Hill, Long Island (L6).

Figure 6. Box plot (central horizontal line = median; shaded box = interquartile range (IQR); whiskers = 1.5 x IQR) of the  $^{87}\text{Sr}/^{86}\text{Sr}$  ratios from the Bahamas and TCI. Created in BoxPlotR (Spitzer et al., 2014).

Figure 7. Predicted Sr isotope ratios for the circum-Caribbean region from the three-source mixing model (after Bataille et al., 2012, Figure 5B). Data sources: Circum-Caribbean Sr isotopes (Bowen, 2017; Lehnert et al., 2000) and The GEBCO\_2014 Grid, version 20150318, [www.gebco.net](http://www.gebco.net).

Figure 8. Histograms showing the difference between the modelled  $^{87}\text{Sr}/^{86}\text{Sr}$  isotope ratios for the Bahamian archipelago from Bataille et al. (2012), based on a three-source mixing model which over-estimates the contribution of Saharan dust, and the results obtained on modern trees in this paper.

Figure 9. Histograms showing the difference between the modelled  $^{87}\text{Sr}/^{86}\text{Sr}$  isotope ratios for Tobago from Bataille et al. (2012), based on a three-source mixing model which over-estimates the contribution of Saharan dust, and Ostapkowicz et al. (2017), based on Empirical Bayesian Kriging of measured values from modern plant samples.

Table 1

| <i>Island</i> | <i>Group</i> | <i>Species</i>            | <i>Map</i> | <i>Sample id</i> | $^{87}\text{Sr}/^{86}\text{Sr}$ | <i>Z-score</i> | <i>Latitude</i> | <i>Longitude</i> | <i>masl</i> | <i>Tree size</i> | <i>Location</i> | <i>Soil</i> | <i>Landform</i> |
|---------------|--------------|---------------------------|------------|------------------|---------------------------------|----------------|-----------------|------------------|-------------|------------------|-----------------|-------------|-----------------|
| Eleuthera     | Bahamas      | <i>Guaiacum sanctum</i>   | –          | 09-001           | 0.709183                        | -1.457         | –               | –                | –           | –                | –               | –           |                 |
| Eleuthera     | Bahamas      | <i>Guaiacum sanctum</i>   | –          | 09-002           | 0.709155                        | 1.319          | –               | –                | –           | –                | –               | –           |                 |
| Long Island   | Bahamas      | <i>Guaiacum sanctum</i>   | L1         | 09-003           | 0.709175                        | -0.621         | 22.87478        | -74.86753        | 10          | med              | coastal         | Coral       | Plane           |
| Long Island   | Bahamas      | <i>Guaiacum sanctum</i>   | L2         | 09-004           | 0.709170                        | -0.142         | 22.92033        | -74.88619        | 5           | large            | inland          | Coral       | Plane           |
| Long Island   | Bahamas      | <i>Guaiacum sanctum</i>   | L3         | 09-005           | 0.709169                        | -0.069         | 23.00236        | -74.88794        | 9           | small            | inland          | Swamp       | Plane           |
| Long Island   | Bahamas      | <i>Guaiacum sanctum</i>   | L4         | 09-006           | 0.709169                        | -0.038         | 23.06525        | -74.92806        | 8           | small            | inland          | Red         | Plane           |
| Long Island   | Bahamas      | <i>Guaiacum sanctum</i>   | L5         | 09-007           | 0.709164                        | 0.429          | 23.09194        | -75.12017        | 18          | large            | coastal         | Coral       | Ridge           |
| Long Island   | Bahamas      | <i>Guaiacum sanctum</i>   | L6         | 09-008           | 0.709173                        | -0.412         | 23.09689        | -75.02117        | 9           | med              | inland          | Red         | Plane           |
| Long Island   | Bahamas      | <i>Swietenia mahagoni</i> | L7         | 09-009           | 0.709157                        | 1.166          | 23.12081        | -75.05281        | 7           | med              | coastal         | Coral       | Plane           |
| Long Island   | Bahamas      | <i>Swietenia mahagoni</i> | L8         | 09-010           | 0.709169                        | -0.061         | 23.17117        | -75.10114        | 6           | med              | inland          | Black       | Plane           |
| Long Island   | Bahamas      | <i>Guaiacum sanctum</i>   | L9         | 09-011           | 0.709159                        | 0.962          | 23.20539        | -75.10681        | 9           | med              | inland          | Black       | Plane           |
| Long Island   | Bahamas      | <i>Swietenia mahagoni</i> | L10        | 09-012           | 0.709163                        | 0.580          | 23.25233        | -75.10308        | 4           | med              | coastal         | Black       | Plane           |
| Long Island   | Bahamas      | <i>Guaiacum sanctum</i>   | L11        | 09-013           | 0.709181                        | -1.229         | 23.28922        | -75.10383        | 12          | med              | inland          | Black       | Plane           |
| Long Island   | Bahamas      | <i>Guaiacum sanctum</i>   | L12        | 09-014           | 0.709162                        | 0.632          | 23.33389        | -75.11992        | 11          | small            | coastal         | Black       | Plane           |
| Long Island   | Bahamas      | <i>Swietenia mahagoni</i> | L13        | 09-015           | 0.709171                        | -0.237         | 23.38131        | -75.14369        | 8           | med              | coastal         | Black       | Plane           |
| Long Island   | Bahamas      | <i>Guaiacum sanctum</i>   | L14        | 09-016           | 0.709160                        | 0.824          | 23.66547        | -75.31228        | 7           | small            | inland          | Black       | Plane           |
| Long Island   | Bahamas      | <i>Swietenia mahagoni</i> | L15        | 09-017           | 0.709180                        | -1.127         | 23.62439        | -75.29589        | 2           | med              | coastal         | Coral       | Plane           |
| Long Island   | Bahamas      | <i>Guaiacum sanctum</i>   | L16        | 09-018           | 0.709157                        | 1.165          | 23.55958        | -75.25328        | 5           | large            | coastal         | Black       | Plane           |
| Long Island   | Bahamas      | <i>Swietenia mahagoni</i> | L17        | 09-019           | 0.709164                        | 0.475          | 23.55603        | -75.25703        | 3           | med              | inland          | Black       | Plane           |
| Long Island   | Bahamas      | <i>Guaiacum sanctum</i>   | L18        | 09-020           | 0.709185                        | -1.576         | 23.52136        | -75.24961        | 11          | large            | inland          | Black       | Ridge           |
| Long Island   | Bahamas      | <i>Guaiacum sanctum</i>   | L19        | 09-021           | 0.709173                        | -0.433         | 23.45231        | -75.21642        | 6           | med              | inland          | Coral       | Plane           |
| Long Island   | Bahamas      | <i>Guaiacum sanctum</i>   | L20        | 09-022           | 0.709170                        | -0.166         | 23.41817        | -75.18603        | 8           | large            | coastal         | Black       | Plane           |
| Cat Island    | Bahamas      | <i>Swietenia mahagoni</i> | C1         | 09-023           | 0.709167                        | 0.166          | 24.60456        | -75.65319        | 0           | small            | coastal         | Red         | Plane           |
| Cat Island    | Bahamas      | <i>Swietenia mahagoni</i> | C2         | 09-024           | 0.709166                        | 0.264          | 24.52508        | -75.59486        | 1           | small            | coastal         | Black       | Plane           |
| Cat Island    | Bahamas      | <i>Swietenia mahagoni</i> | C3         | 09-025           | 0.709171                        | -0.211         | 24.45044        | -75.54706        | 5           | med              | coastal         | Red         | Plane           |
| Cat Island    | Bahamas      | <i>Swietenia mahagoni</i> | C4         | 09-026           | 0.709179                        | -1.014         | 24.34486        | -75.48083        | 10          | med              | coastal         | Black       | Plane           |
| Cat Island    | Bahamas      | <i>Swietenia mahagoni</i> | C5         | 09-027           | 0.709175                        | -0.643         | 24.27172        | -75.40336        | 7           | small            | coastal         | Black       | Plane           |
| Cat Island    | Bahamas      | <i>Swietenia mahagoni</i> | C6         | 09-028           | 0.709177                        | -0.852         | 24.20833        | -75.38653        | 4           | small            | inland          | Swamp       | Plane           |
| Cat Island    | Bahamas      | <i>Swietenia mahagoni</i> | C7         | 09-029           | 0.709166                        | 0.316          | 24.16467        | -75.40558        | 3           | small            | inland          | Black       | Plane           |
| Cat Island    | Bahamas      | <i>Swietenia mahagoni</i> | C8         | 09-030           | 0.709168                        | 0.120          | 24.14136        | -75.45728        | 7           | small            | inland          | Black       | Plane           |
| Cat Island    | Bahamas      | <i>Guaiacum sanctum</i>   | C9         | 09-031           | 0.709169                        | -0.024         | 24.14333        | -75.43706        | 21          | small            | coastal         | Black       | Ridge           |
| Cat Island    | Bahamas      | <i>Swietenia mahagoni</i> | C10        | 09-032           | 0.709177                        | -0.816         | 24.18242        | -75.31803        | 12          | med              | inland          | Coral       | Ridge           |
| Cat Island    | Bahamas      | <i>Guaiacum sanctum</i>   | C11        | 09-033           | 0.709166                        | 0.261          | 24.17364        | -75.31592        | 19          | small            | inland          | Coral       | Ridge           |

|                |         |                              |     |         |          |        |          |           |    |       |         |       |         |
|----------------|---------|------------------------------|-----|---------|----------|--------|----------|-----------|----|-------|---------|-------|---------|
| Cat Island     | Bahamas | <i>Guaiacum sanctum</i>      | C12 | 09-034  | 0.709171 | -0.252 | 24.17492 | -75.31669 | 23 | med   | inland  | Coral | Ridge   |
| Cat Island     | Bahamas | <i>Guaiacum sanctum</i>      | C13 | 09-035  | 0.709174 | -0.541 | 24.19692 | -75.33981 | 13 | med   | inland  | Black | Plane   |
| Cat Island     | Bahamas | <i>Swietenia mahagoni</i>    | C14 | 09-036  | 0.709174 | -0.492 | 24.21947 | -75.35556 | 20 | small | inland  | Red   | Channel |
| Cat Island     | Bahamas | <i>Lysiloma latisiliquum</i> | C15 | 09-037  | 0.709176 | -0.768 | 24.17492 | -75.31669 | 23 | large | inland  | Coral | Ridge   |
| Providenciales | TCI     | <i>Guaiacum officinale</i>   | -   | BNM 412 | 0.709166 | 0.245  | -        | -         | -  | -     | -       | -     | -       |
| Providenciales | TCI     | <i>Guaiacum sanctum</i>      | P1  | BNM 419 | 0.709174 | -0.539 | 21.79413 | -72.17587 | 8  | large | coastal |       | Plane   |
| Providenciales | TCI     | <i>Zanthoxylum flavum</i>    | P2  | BNM 420 | 0.709166 | 0.244  | 21.79413 | -72.17587 | 8  | med   | coastal |       | Plane   |
| Providenciales | TCI     | <i>Swietenia mahagoni</i>    | P3  | BNM 421 | 0.709158 | 1.045  | 21.83880 | -72.32998 | 9  | large | coastal |       | Plane   |
| Providenciales | TCI     | <i>Guaiacum sanctum</i>      | P4  | BNM 422 | 0.709198 | -2.912 | 21.83880 | -72.32998 | 9  | small | coastal |       | Plane   |
| Providenciales | TCI     | <i>Guaiacum sanctum</i>      | P5  | BNM 423 | 0.709171 | -0.201 | 21.81352 | -72.28062 | 8  | large | coastal |       | Plane   |
| Providenciales | TCI     | <i>Guaiacum sanctum</i>      | P6  | BNM 424 | 0.709162 | 0.630  | 21.74917 | -72.26825 | 7  | small | coastal |       | Plane   |
| Providenciales | TCI     | <i>Zanthoxylum flavum</i>    | P7  | BNM 425 | 0.709174 | -0.491 | 21.77740 | -72.17172 | 20 | med   | coastal |       | Ridge   |
| Providenciales | TCI     | <i>Guaiacum sanctum</i>      | P8  | BNM 426 | 0.709163 | 0.555  | 21.76381 | -72.17104 | 20 | med   | coastal |       | Ridge   |
| Providenciales | TCI     | <i>Guaiacum sanctum</i>      | P9  | BNM 427 | 0.709161 | 0.775  | 21.76381 | -72.17104 | 20 | med   | coastal |       | Ridge   |
| Providenciales | TCI     | <i>Swietenia mahagoni</i>    | P10 | BNM 428 | 0.709164 | 0.456  | 21.78672 | -72.16900 | 7  | large | coastal |       | Plane   |
| Providenciales | TCI     | <i>Guaiacum sanctum</i>      | P11 | BNM 429 | 0.709149 | 1.955  | 21.78042 | -72.25175 | 14 | large | coastal |       | Plane   |
| North Caicos   | TCI     | <i>Swietenia mahagoni</i>    | N1  | BNM 444 | 0.709167 | 0.172  | 21.83683 | -71.88733 | 6  | small | inland  |       | Plane   |
| North Caicos   | TCI     | <i>Swietenia mahagoni</i>    | N2  | BNM 445 | 0.709135 | 3.332  | 21.83783 | -71.90117 | 7  | small | inland  |       | Plane   |
| North Caicos   | TCI     | <i>Guaiacum sanctum</i>      | N3  | BNM 446 | 0.709175 | -0.641 | 21.89217 | -71.92083 | 7  | large | coastal |       | Plane   |
| North Caicos   | TCI     | <i>Guaiacum sanctum</i>      | N4  | BNM 447 | 0.709165 | 0.381  | 21.93700 | -72.03750 | 7  | med   | coastal |       | Plane   |
| North Caicos   | TCI     | <i>Cordia sebestina</i>      | N5  | BNM 448 | 0.709187 | -1.838 | 21.93717 | -72.03717 | 8  | med   | coastal |       | Plane   |
| North Caicos   | TCI     | <i>Guaiacum sanctum</i>      | N6  | BNM 449 | 0.709162 | 0.639  | 21.93717 | -72.03650 | 8  | large | inland  |       | Plane   |
| North Caicos   | TCI     | <i>Swietenia mahagoni</i>    | N7  | BNM 450 | 0.709171 | -0.270 | 21.93683 | -72.02200 | 11 | med   | inland  |       | Channel |
| North Caicos   | TCI     | <i>Swietenia mahagoni</i>    | N8  | BNM 451 | 0.709182 | -1.279 | 21.92467 | -71.98750 | 10 | large | coastal |       | Plane   |
| North Caicos   | TCI     | <i>Guaiacum sanctum</i>      | N9  | BNM 452 | 0.709162 | 0.651  | 21.93170 | -71.97722 | 11 | small | inland  |       | Plane   |
| North Caicos   | TCI     | <i>Swietenia mahagoni</i>    | N10 | BNM 453 | 0.709168 | 0.056  | 21.93170 | -71.97722 | 7  | large | inland  |       | Channel |
| North Caicos   | TCI     | <i>Guaiacum sanctum</i>      | N11 | BNM 454 | 0.709177 | -0.789 | 21.92037 | -71.92178 | 9  | small | inland  |       | Plane   |
| North Caicos   | TCI     | <i>Guaiacum sanctum</i>      | N12 | BNM 455 | 0.709170 | -0.103 | 21.91883 | -71.92647 | 7  | large | inland  |       | Plane   |
| North Caicos   | TCI     | <i>Swietenia mahagoni</i>    | N13 | BNM 456 | 0.709167 | 0.174  | 21.92183 | -71.92600 | 7  | large | inland  |       | Plane   |
| North Caicos   | TCI     | <i>Swietenia mahagoni</i>    | N14 | BNM 457 | 0.709168 | 0.059  | 21.93170 | -71.97722 | 6  | med   | coastal |       | Plane   |
| North Caicos   | TCI     | <i>Guaiacum sanctum</i>      | N15 | BNM 458 | 0.709162 | 0.671  | 21.94050 | -71.95133 | 6  | med   | coastal |       | Plane   |
| North Caicos   | TCI     | <i>Swietenia mahagoni</i>    | N16 | BNM 459 | 0.709168 | 0.072  | 21.90550 | -72.03633 | 7  | large | coastal |       | Plane   |
| North Caicos   | TCI     | <i>Guaiacum sanctum</i>      | N17 | BNM 460 | 0.709184 | -1.497 | 21.91833 | -72.00817 | 14 | small | coastal |       | Ridge   |
| North Caicos   | TCI     | <i>Swietenia mahagoni</i>    | N18 | BNM 461 | 0.709163 | 0.610  | 21.91817 | -72.00567 | 4  | large | coastal |       | Plane   |

|               |     |                            |     |         |          |        |          |           |    |       |         |              |
|---------------|-----|----------------------------|-----|---------|----------|--------|----------|-----------|----|-------|---------|--------------|
| North Caicos  | TCI | <i>Swietenia mahagoni</i>  | N19 | BNM 462 | 0.709176 | -0.697 | 21.90333 | -72.00100 | 9  | large | coastal | Plane        |
| North Caicos  | TCI | <i>Guaiacum sanctum</i>    | N20 | BNM 463 | 0.709163 | 0.588  | 21.95050 | -72.03533 | 6  | large | inland  | Plane        |
| North Caicos  | TCI | <i>Swietenia mahagoni</i>  | N21 | BNM 464 | 0.709165 | 0.402  | 21.95000 | -72.03467 | 11 | med   | coastal | Plane        |
| Middle Caicos | TCI | <i>Zanthoxylum flavum</i>  | M1  | BNM 430 | 0.709158 | 1.101  | 21.81255 | -71.66547 | 12 | small | inland  | Plane        |
| Middle Caicos | TCI | <i>Swietenia mahagoni</i>  | M2  | BNM 431 | 0.709170 | -0.159 | 21.82350 | -71.67857 | 12 | med   | coastal | Plane        |
| Middle Caicos | TCI | <i>Guaiacum sanctum</i>    | M3  | BNM 432 | 0.709168 | 0.115  | 21.81933 | -71.67617 | 12 | med   | coastal | Plane        |
| Middle Caicos | TCI | <i>Swietenia mahagoni</i>  | M4  | BNM 433 | 0.709163 | 0.539  | 21.81933 | -71.67617 | 6  | med   | inland  | Plane        |
| Middle Caicos | TCI | <i>Guaiacum sanctum</i>    | M5  | BNM 434 | 0.709154 | 1.493  | 21.81900 | -71.68450 | 11 | med   | inland  | Plane        |
| Middle Caicos | TCI | <i>Guaiacum sanctum</i>    | M6  | BNM 435 | 0.709176 | -0.675 | 21.81900 | -71.68417 | 13 | small | coastal | Plane        |
| Middle Caicos | TCI | <i>Guaiacum sanctum</i>    | M7  | BNM 436 | 0.709169 | -0.013 | 21.78917 | -71.68667 | 12 | med   | inland  | Red<br>Plane |
| Middle Caicos | TCI | <i>Guaiacum sanctum</i>    | M8  | BNM 437 | 0.709170 | -0.137 | 21.80700 | -71.72000 | 3  | med   | inland  | Plane        |
| Middle Caicos | TCI | <i>Cordia sebestina</i>    | M9  | BNM 438 | 0.709174 | -0.500 | 21.82333 | -71.73483 | 3  | large | inland  | Plane        |
| Middle Caicos | TCI | <i>Swietenia mahagoni</i>  | M10 | BNM 439 | 0.709165 | 0.409  | 21.82583 | -71.77533 | 15 | med   | inland  | Plane        |
| Middle Caicos | TCI | <i>Swietenia mahagoni</i>  | M11 | BNM 440 | 0.709175 | -0.672 | 21.82017 | -71.77217 | 11 | large | inland  | Plane        |
| Middle Caicos | TCI | <i>Swietenia mahagoni</i>  | M12 | BNM 441 | 0.709165 | 0.350  | 21.81850 | -71.75150 | 5  | med   | coastal | Red<br>Plane |
| Middle Caicos | TCI | <i>Swietenia mahagoni</i>  | M13 | BNM 442 | 0.709190 | -2.160 | 21.81850 | -71.75150 | 6  | small | coastal | Plane        |
| Middle Caicos | TCI | <i>Guaiacum sanctum</i>    | M14 | BNM 443 | 0.709142 | 2.610  | 21.82567 | -71.80617 | 4  | small | inland  | Plane        |
| East Caicos   | TCI | <i>Zanthoxylum flavum</i>  | E1  | BNM 465 | 0.709155 | 1.349  | 21.73800 | -71.59217 | 8  | med   | coastal | Plane        |
| East Caicos   | TCI | <i>Guaiacum sanctum</i>    | E2  | BNM 466 | 0.709186 | -1.759 | 21.73800 | -71.59217 | 8  | med   | coastal | Plane        |
| East Caicos   | TCI | <i>Guaiacum sanctum</i>    | E3  | BNM 467 | 0.709183 | -1.419 | 21.73800 | -71.59217 | 8  | small | coastal | Plane        |
| East Caicos   | TCI | <i>Guaiacum officinale</i> | E4  | BNM 468 | 0.709152 | 1.620  | 21.73783 | -71.59083 | 9  | small | coastal | Plane        |
| East Caicos   | TCI | <i>Guaiacum officinale</i> | E5  | BNM 469 | 0.709149 | 1.986  | 21.73800 | -71.59100 | 10 | small | coastal | Plane        |
| East Caicos   | TCI | <i>Guaiacum officinale</i> | E6  | BNM 470 | 0.709179 | -1.003 | 21.73817 | -71.59117 | 10 | -     | coastal | Plane        |
| East Caicos   | TCI | <i>Swietenia mahagoni</i>  | E7  | BNM 471 | 0.709179 | -1.028 | 21.73817 | -71.59133 | 8  | -     | coastal | Plane        |

Table 2

| <i>Island</i>             | $^{87}\text{Sr}/^{86}\text{Sr}$ | $\pm$    | <i>maximum</i> | <i>minimum</i> | <i>n</i> |
|---------------------------|---------------------------------|----------|----------------|----------------|----------|
| <i>Bahamas</i>            |                                 |          |                |                |          |
| Eleuthera                 | 0.709169                        | 0.000020 | 0.709183       | 0.709155       | 2        |
| Cat Island                | 0.709172                        | 0.000002 | 0.709179       | 0.709166       | 15       |
| Long Island               | 0.709169                        | 0.000008 | 0.709186       | 0.709149       | 20       |
| <i>Turks &amp; Caicos</i> |                                 |          |                |                |          |
| Providenciales            | 0.709169                        | 0.000012 | 0.709198       | 0.709149       | 12       |
| North Caicos              | 0.709168                        | 0.000011 | 0.709187       | 0.709135       | 21       |
| Middle Caicos             | 0.709167                        | 0.000011 | 0.709190       | 0.709142       | 14       |
| East Caicos               | 0.709169                        | 0.000016 | 0.709185       | 0.709157       | 7        |
| <i>Total</i>              | 0.709169                        | 0.000010 | 0.709198       | 0.709135       | 91       |

Figure 1

[Click here to download Figure Schulting\\_et\\_al\\_Figure\\_1.png](#)

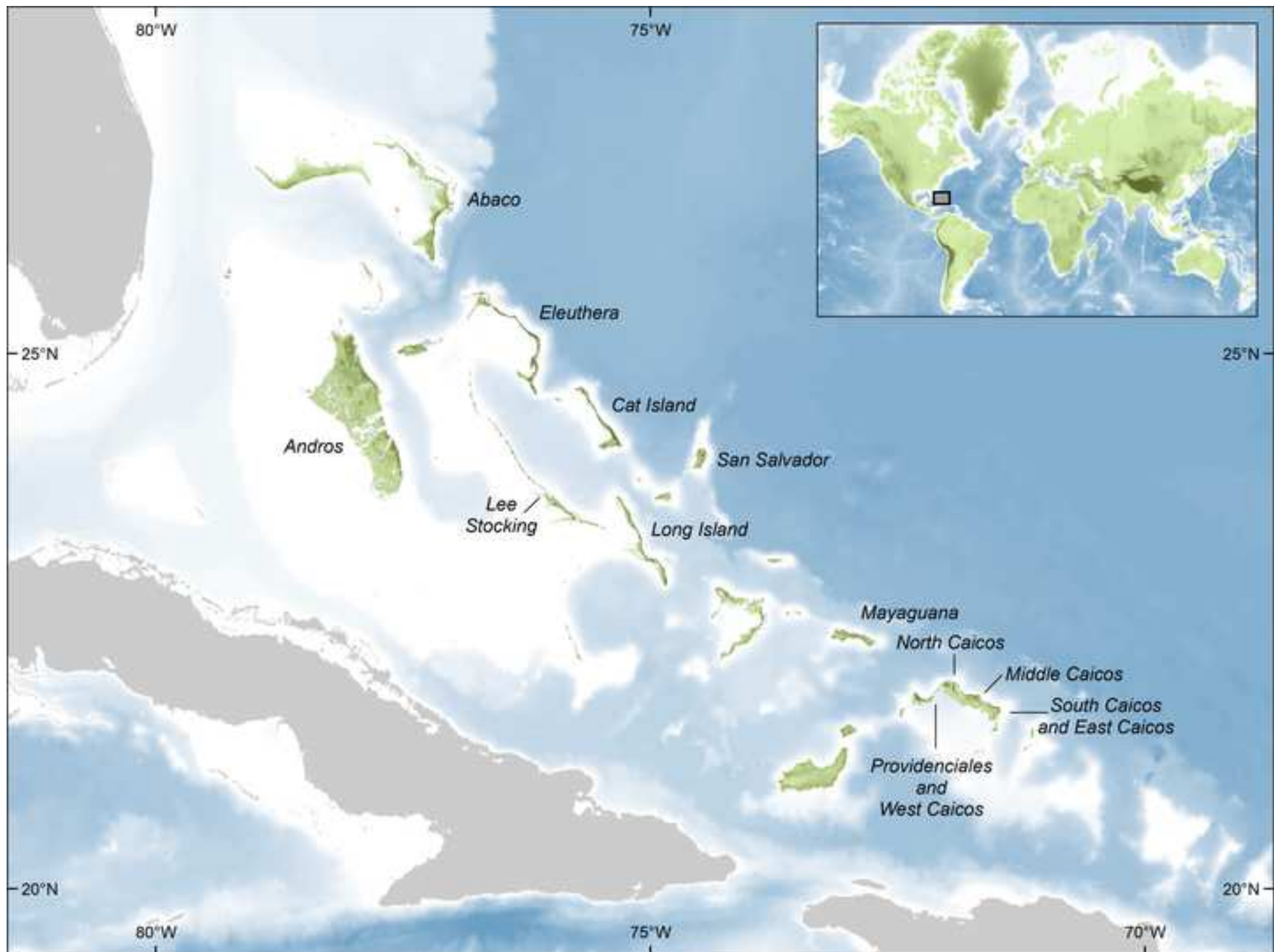




Figure 2a



Figure 2b



Figure 3a

[Click here to download Figure Schulting\\_et\\_al\\_Figure\\_3a.png](#)







Figure 4

[Click here to download Figure Schulting\\_et\\_al\\_Figure\\_4.png](#)

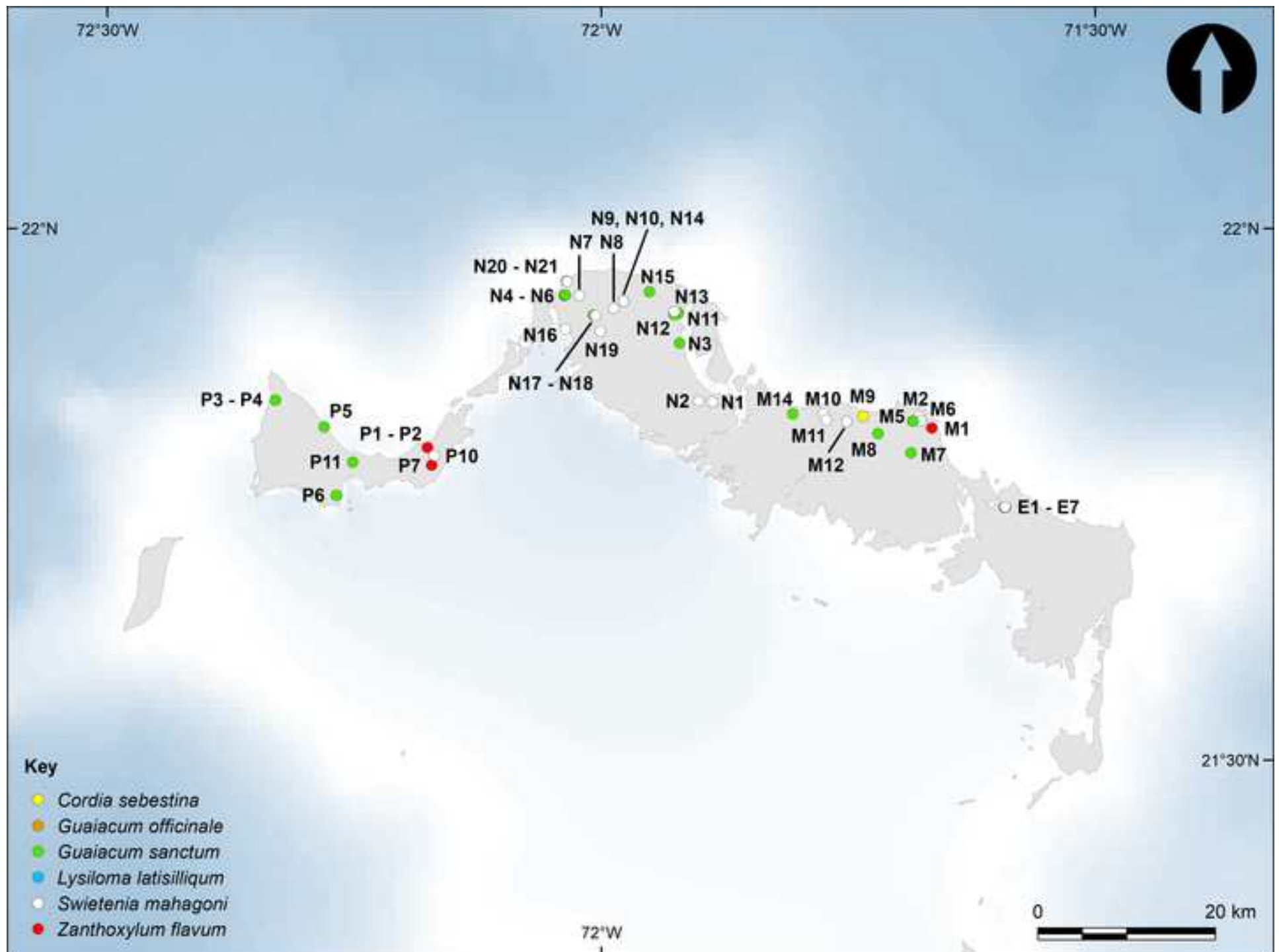




Figure 5

[Click here to download Figure Schulting\\_et\\_al\\_Figure\\_5\\_soils.jpg](#)



Figure 6

[Click here to download Figure Schulting\\_et\\_al\\_Figure\\_6.pdf](#)

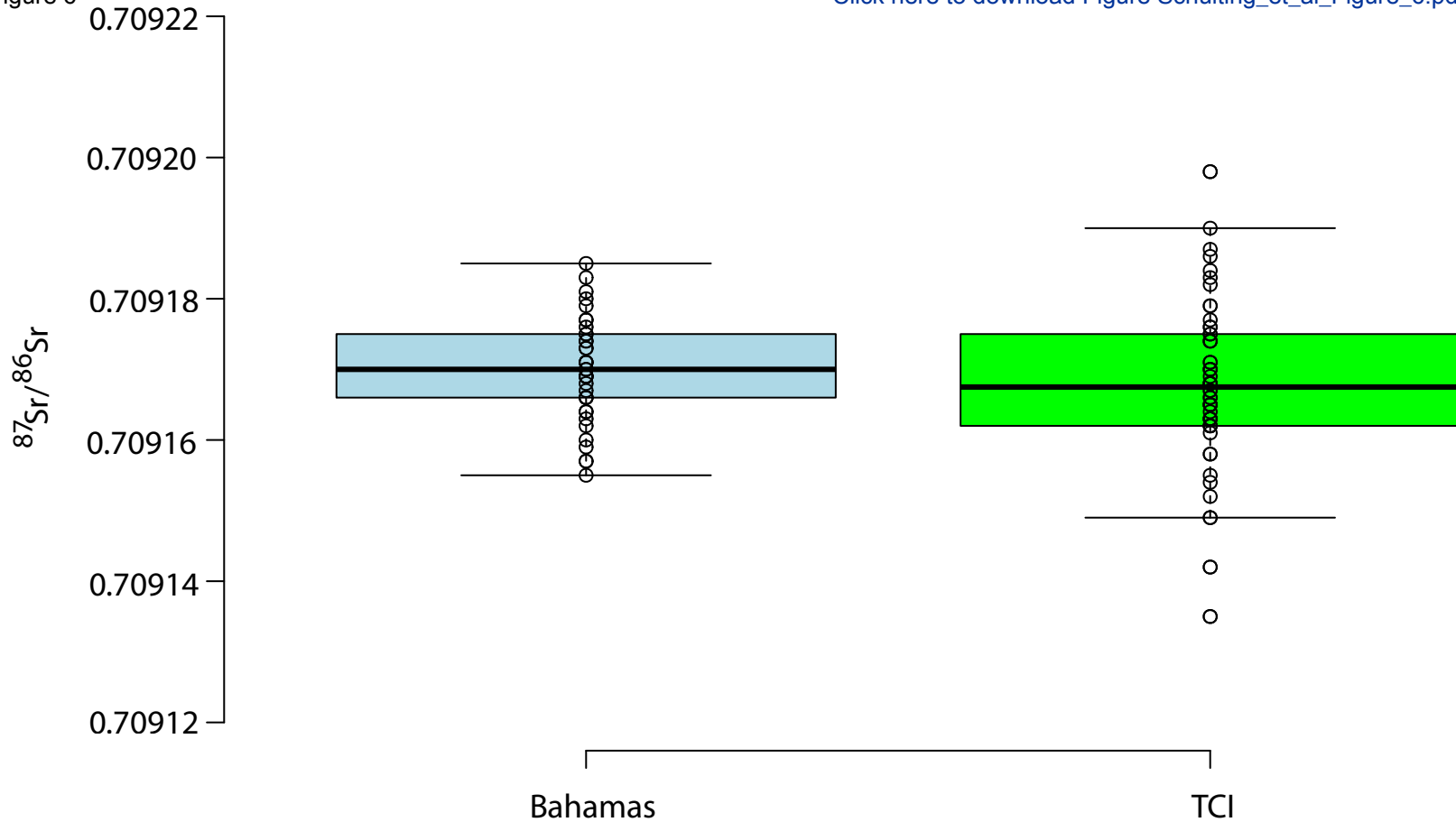




Figure 7

[Click here to download Figure Schulting\\_et\\_al\\_Figure\\_7.png](#)

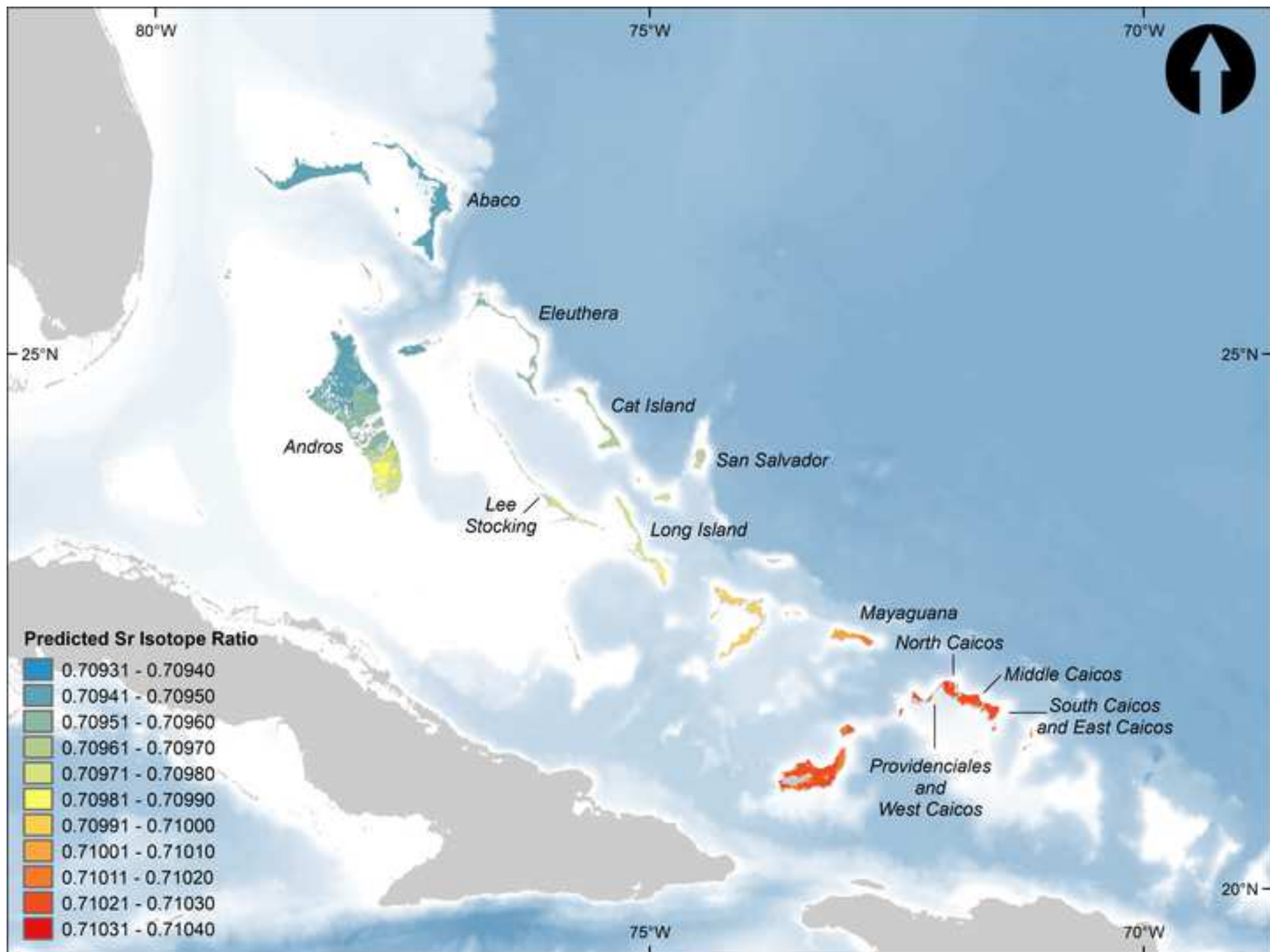




Figure 8

[Click here to download Figure Schulting\\_et\\_al\\_Figure\\_8.png](#)

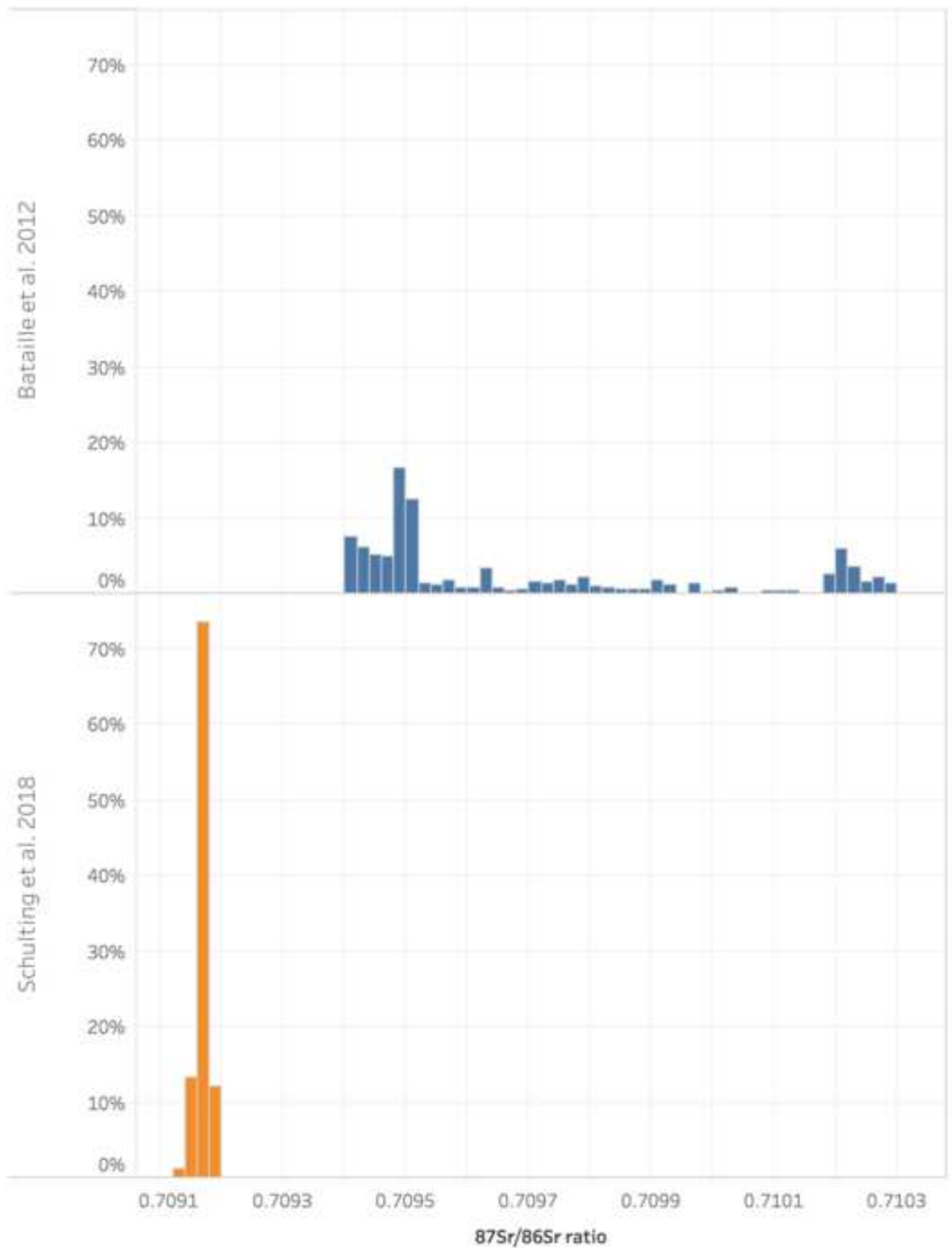


Figure 9

[Click here to download Figure Schulting\\_et\\_al\\_Figure\\_9.png](#)

